Award Number: W81XWH-13-1-0325

TITLE: Developing Novel Therapeutic Approaches in Small Cell Lung Carcinoma Using Genetically Engineered Mouse Models and Human Circulating Tumor Cells

PRINCIPAL INVESTIGATOR: Jeffrey Engelman MD PhD

CONTRACTING ORGANIZATION: Massachusetts General Hospital
Boston MA 02114-2621

REPORT DATE: December 2016

TYPE OF REPORT: Final

PREPARED FOR: U.S. Army Medical Research and Materiel Command
Fort Detrick, Maryland 21702-5012

REPORT DOCUMENTATION PAGE

Form Approved
OMB No. 0704-0188

1. REPORT DATE *(DD-MM-YYYY)*	**2. REPORT TYPE**	**3. DATES COVERED** *(From - To)*
December 2016	Final	15Sep2013 - 14Sep2016

4. TITLE AND SUBTITLE

Developing Novel Therapeutic Approaches in Small Cell Lung Carcinoma Using Genetically Engineered Mouse Models and Human Circulating Tumor Cells

5a. CONTRACT NUMBER
W81XWH-13-1-0325

5b. GRANT NUMBER
LC120307P1

5c. PROGRAM ELEMENT NUMBER

6. AUTHOR(S)
Jeffrey Engelman MD PhD

Email: jengelman@partners.org

5d. PROJECT NUMBER

5e. TASK NUMBER

5f. WORK UNIT NUMBER

7. PERFORMING ORGANIZATION NAME(S) AND ADDRESS(ES)

Massachusetts General Hospital
55 Fruit St
Boston MA 02114

8. PERFORMING ORGANIZATION REPORT NUMBER

9. SPONSORING / MONITORING AGENCY NAME(S) AND ADDRESS(ES)
US Army Medical Research and Materiel Command
Fort Detrick, MD 21702-5012

10. SPONSOR/MONITOR'S ACRONYM(S)

11. SPONSOR/MONITOR'S REPORT NUMBER(S)

12. DISTRIBUTION / AVAILABILITY STATEMENT

Approved for Public Release; Distribution Unlimited

13. SUPPLEMENTARY NOTES

14. ABSTRACT

We have successfully developed mouse models in which to perform in vivo experiments, as well as developed expertise in live animal imaging to enable monitoring to tumors over time in these models. We have initiated treatment studies with chemotherapy and with targeted therapies in our models. Our preliminary data indicate that tumor response to chemotherapy in our models is modest. However, we find that tumor response to combination targeted therapy is significantly superior to either targeted therapy alone or to no treatment. Correlative biomarker studies are underway, including the isolation and enumeration of circulating tumor cells from SCLC patients. These findings support further development of this combination therapy approach and we anticipate ongoing experiments to assess correlative biomarkers.

15. SUBJECT TERMS
Small cell lung cancer (SCLC), Genetically engineered mouse model (GEMM), BH3 mimetic, TORC inhibitor, Apoptosis, Preclinical therapeutics

16. SECURITY CLASSIFICATION OF:			**17. LIMITATION OF ABSTRACT**	**18. NUMBER OF PAGES**	**19a. NAME OF RESPONSIBLE PERSON**
a. REPORT	**b. ABSTRACT**	**c. THIS PAGE**			USAMRMC
Unclassified	Unclassified	Unclassified	UU	49	**19b. TELEPHONE NUMBER** *(include area code)*

Standard Form 298 (Rev. 8-98)
Prescribed by ANSI Std. Z39.18

Table of Contents

INTRODUCTION

Small cell lung cancer (SCLC) is an aggressive neuroendocrine carcinoma with a median survival of less than one year and a five-year overall survival of under 2% in the metastatic setting. While chemotherapy initially induces a response in most patients, metastatic disease invariably recurs rapidly and is often resistant to additional conventional therapies. To date, there are no effective targeted therapeutic approaches in SCLC and research efforts to develop new therapeutic strategies for these cancers have lagged far behind those for non-small cell lung cancer. This project aims to address these fundamental challenges by utilizing genetically engineered mouse models (GEMMs) of SCLC that faithfully recapitulate the human disease, as well as circulating tumor cells (CTCs) from both the GEMMs and human SCLC patients to develop a new therapeutic approach. Our therapeutic strategy, the combination of a BH3-mimetic and an mTOR complex (TORC) catalytic site inhibitor, is based on our understanding of the mechanisms of apoptosis and growth arrest in SCLC tumors. Our project aims to (1) explore the mechanism of chemotherapy response and resistance in the GEMM, (2) investigate the activity of combination BH3-mimetic and TORC inhibition therapy in the GEMM, and (3) utilize patient-derived CTCs to monitor treatment response. This report reviews our progress during the third year of funding.

KEYWORDS

Small cell lung cancer (SCLC)
Genetically engineered mouse model (GEMM) BH3 mimetic
TORC inhibitor Apoptosis
Preclinical therapeutics

ACCOMPLISHMENTS

Major goals of the project Specific Aims:

Specific Aim 1: Determine biomarkers of response and resistance to standard chemotherapy in SCLC GEMMs.
Specific Aim 2: Perform preclinical study of combination targeted therapy in SCLC GEMMs.
Specific Aim 3: Utilize patient-derived CTCs as a means to monitor treatment response and predict sensitivity to treatment.

Major Tasks (as detailed in the Statement of Work, modified 9/22/14):

Please see Appendix 1, Statement of Work for MGH.

1. Analyze CTCs from SCLC patients at MGH enrolled on DF/HCC protocol 05-300

Accomplishments under these goals

- **Major Task 8:** The goal of this task is to analyze CTCs from patients with SCLC to assess for changes in CTC number and expression of markers relevant to our combination treatment strategy (P-4EBP1, P-S6, BIM, Bcl-2, Bcl-xL, and Mcl-1 using ISH and IHC) over the course of chemotherapy treatments.

  This work will be performed entirely at MGH under the direction of Dr. Engelman. As we described in a prior

PDX	Prior Tx's	PDX source	P0 latency	Seq
MGH1501	0	CTC	76	
MGH1504	0	CTC	160	P
MGH1505-2	4	CTC	108	
MGH1506	1	CTC	133	
MGH1508	4	CTC	201	
MGH1512-A	2	Bx	60	
MGH1512-B	2	Bx	64	P
MGH1514	0	CTC	130	P
MGH1514-2A	2	Bx	150	
MGH1514-2B	2	CTC	229	
MGH1514-5	5	Bx	59	
MGH1515	2	CTC	108	P
MGH1517	0	Bx	145	
MGH1518-B	0	Bx	127	
MGH1518-C	0	Bx	81	P
MGH1518-3A	2	Bx	38	
MGH1520	0	CTC	236	
MGH1521-A	0	CTC	74	
MGH1522	0	Bx	54	
MGH1523-A	0	CTC	223	
MGH1524	0	CTC	83	
MGH1525	0	CTC	45	P
MGH1528	6	CTC	107	P
MGH1528-2	7	CTC	115	
MGH1529	1	Bx	98	
MGH1531-B	1	Eff	55	
MGH1534	1	Bx	94	
MGH1535	1	Bx	81	
MGH1536	2	Bx	75	
MGH1537	1	Bx	71	
MGH1538-B	1	Bx	78	
MGH1541	0	Eff	74	
MGH1543	2	CTC	83	
MGH1545-A	1	Bx	25	
MGH1545-B	1	Bx	25	
MGH1545-C	1	CTC	30	

Table 1: MGH SCLC PDX models. Deeper colors = Progressive time points during treatment course. Prior Tx: number of lines of therapy. Bx: biopsy. P0 latancy: Time from tissue implantation to detection of palpable tumor. Seq = P: undergoing whole exome sequencing and RNAseq.

submission requesting changes to the Statement of Work, Dr. Engelman's group has proposed what we believe to be an improved approach for accomplishing this task. The original grant proposal had described accomplishing this Aim by using the herringbone chip (Maheswaran et al., 2008; Nagrath et al., 2007; Yu et al., 2012). This technology captures cells to a device and allows for enumeration and IHC and in-situ hybridization (ISH) on CTCs, but does not enable collection or propagation of live CTCs. Recently, the Haber and Toner labs at MGH have developed a microfluidic-based live CTC capture platform, the CTC-iChip (Karabacak et al., 2014; Ozkumur et al., 2013). Using antigen-based removal of leukocytes and granulocytes, this technology enables unbiased collection of unperturbed live CTCs in suspension. The Engelman group now proposes to leverage CTC-iChip technology to generate mouse xenograft models directly from SCLC CTCs. Generation of SCLC "CTC-derived xenografts" (CDXs) has recently been described (Hodgkinson et al., 2014). The Engelman group proposes generate xenografts in a similar manner. CTC enrichment from whole blood will be performed using the ^{neg}CTC-iChip and ^{pos}CTC-iChip platforms (Karabacak et al., 2014; Ozkumur et al., 2013). They will quantify the number of enriched CTCs per mL of whole blood using histologic stains and neuroendocrine marker immunofluorescence. Collected CTCs in suspension will then be mixed with an equal volume of matrigel and directly transplanted subcutaneously (SC) into the flanks of NOD/SCID mice that lack the interleukin-2 gamma receptor (NSG mice) (Quintana et al., 2012; Quintana et al., 2008). They will measure tumor dimensions at least three times weekly to determine the efficiency and kinetics of CDX generation. They will utilize these CDX models to perform the molecular analyses outlined in the original proposal. CDX tumors from CTCs isolated before and after chemotherapy treatment will be interrogated for relative expression of TORC1 pathway mediators (P-S6, P-4EBP1) and apoptosis mediators (Bcl-2, Bcl-xL, BIM, Mcl-1) to determine if measurement of these molecular markers will be informative in clinical development of this novel therapy. Notably, the overall enrollment goal has been reduced to 20 patients given the added resources needed for taking the approach detailed above.

The progress to date is shown in the adjoining table. We have successfully isolated CTCs from several SCLC patients. The injection of these CTCs into mice is not currently being supported by the DOD grant but is shown to demonstrate feasibility. Development of these PDX models has progressed rapidly over the past year, and our panel now includes 36 models derived from both biopsies and CTCs. We have validated these models by immunohistochemistry, and have begun to analyze them genomically by whole exome sequencing. These efforts are not being supported by the DOD grant but demonstrate the promise of our PDX model development program. We are now exploring the functional characteristics of these models by comparing their responses to standard and experimental agents with patient responses. Preliminary results suggest that the PDX models accurately reflect patient responses. In the near future, we are excited to use this panel of PDX models to explore combination therapy targeting Bcl-2 family members and TOR signaling, both to determine overall efficacy and to identify biomarkers of response and resistance.

Opportunities for training and professional development provided by this project Nothing to report

How were the results disseminated to communities of interest?

- Publication: Faber AC, Farago AF, Costa C, Dastur A, Gomez-Caraballo M, Robbins R, Wagner BL, Rideout WM 3rd, Jakubik CT, Ham J, Edelman EJ, Ebi H, Yeo AT, Hata AN, Song Y, Patel NU, March RJ, Tam AT, Milano RJ, Boisvert JL, Hicks MA, Elmiligy S, Malstrom SE, Rivera MN, Harada H, Windle BE, Ramaswamy S, Benes CH, Jacks T, Engelman JA. Assessment of ABT-263 activity across a cancer cell line collection leads to a

potent combination therapy for small-cell lung cancer. Proc Natl Acad Sci U S A. 2015 Mar 17;112(11):E1288-96.

What do you plan to do during the next reporting period to accomplish the goals?

- MGH will perform ongoing CTC collection and analysis from human SCLC patients enrolled on protocol 05-300. The MGH group will also develop CTC-derived xenograft models as described above.

IMPACT

What was the impact on the development of the principal discipline(s) of the project?

Both our study (Faber et al., 2015) and another study (Gardener et al., 2014) assessed the activity of combination Bcl-2 and mTOR inhibition in SCLC and demonstrated strong preclinical activity. Based on these results, clinical investigators on these studies are planning a phase 1/phase 2 study of combination Bcl-2 and mTOR inhibitor therapies. Dr. Hann, Dr. Farago, and Dr. Rudin have submitted a collaborative letter of intent to the Cancer Therapy Evaluation Program (CTEP) at the NCI, and the proposed trial is moving forward in planning stages. This trial will offer a new and innovative therapeutic option for patients with small cell lung cancer.

What is the impact on other disciplines?

Nothing to report.

What was the impact on technology transfer?

Nothing to report.

What was the impact on society beyond science and technology?

Nothing to report.

CHANGES/PROBLEMS

Changes in approach and reasons for change

We have no additional changes to make in our approach beyond what was requested on 9/22/14 and reported in our first annual report.

Actual or anticipated problems or delays and actions or plans to resolve them

The IHC assays performed directly on CTCs did not work well. However, CTC-derived PDX models of SCLC closely resemble the patient tumors. In the future we will use these CTC-derived PDX models to assess the effects of therapeutics on TOR signaling and Bcl-2 family members.

Changes that had a significant impact on expenditures

We have no additional changes to make in our budget expenditures other than what was requested on 9/22/14 and reported in our first annual report.

Significant changes in use or care of human subjects, vertebrate animals, biohazards and/or select agents

We have no additional changes to make in use of vertebrate animals, biohazards and/or select reagents beyond what was requested on 9/22/14 and reported in our first annual report.

PRODUCTS

Publications, conference papers, and presentations

- Published manuscript: Faber AC, Farago AF, Costa C, Dastur A, Gomez-Caraballo M, Robbins R, Wagner BL, Rideout WM 3rd, Jakubik CT, Ham J, Edelman EJ, Ebi H, Yeo AT, Hata AN, Song Y, Patel NU, March RJ, Tam AT, Milano RJ, Boisvert JL, Hicks MA, Elmiligy S, Malstrom SE, Rivera MN, Harada H, Windle BE, Ramaswamy S, Benes CH, Jacks T, Engelman JA. Assessment of ABT-263 activity across a cancer cell line collection leads to a potent combination therapy for small-cell lung cancer. Proc Natl Acad Sci U S A. 2015 Mar 17;112(11):E1288-96

PARTICIPANTS & OTHER COLLABORATING ORGANIZATIONS

- **What individuals have worked on the project?**

Name:	Jeffrey Engelman
Project Role:	PI
Researcher Identifier (e.g. ORCID ID):	No change
Nearest person month worked:	1
Contribution to Project:	No change
Funding Support:	No change
Name:	Erin Sennott
Project Role:	Fellow
Researcher Identifier (e.g. ORCID ID):	No change
Nearest person month worked:	1
Contribution to Project:	Research Fellow
Funding Support:	No change
Name:	Haichuan Hu
Project Role:	Fellow
Researcher Identifier (e.g. ORCID ID):	No change
Nearest person month worked:	12
Contribution to Project:	Research Fellow
Funding Support:	No change
Name:	Erin Silva
Project Role:	Technician
Researcher Identifier (e.g. ORCID ID):	No change
Nearest person month worked:	5
Contribution to Project:	Research Technician
Funding Support:	No change
Name:	Eugene Lifshits
Project Role:	Technologist
Researcher Identifier (e.g. ORCID ID):	No change

Nearest person month worked:	12
Contribution to Project:	Research Technologist
Funding Support:	No change
Name:	Max Greenberg
Project Role:	Technician
Researcher Identifier (e.g. ORCID ID):	No change
Nearest person month worked:	7
Contribution to Project:	Research Technician
Funding Support:	No change
Name:	Hillary Mulvey
Project Role:	Technician
Researcher Identifier (e.g. ORCID ID):	No change
Nearest person month worked:	6
Contribution to Project:	Research Technician
Funding Support:	No change

- **Has there been a change in the active other support of the PD/PI(s) or senior/key personnel since the last reporting period?**

  Dr. Engelman left MGH on July 1 2016.

- **What other organizations were involved as partners?**
  - Nothing to Report.

SPECIAL REPORTING REQUIREMENTS

COLLABORATIVE AWARDS

This project is designed as a collaborative project with Dr. Tylers's group at MIT. We have maintained excellent communication with our collaborators about this project and have revised and published a manuscript over the past year. The progress described in this report reflects work done at MGH.

APPENDICES

1. List of personnel paid from the project.
2. Publication

Personnel Effort on Project

Jeffrey Engelman, Principal Investigator
Erin Sennott, Postdoctoral Fellow
Haichuan Hu, Postdoctoral Fellow
Luc Friboulet, Postdoctoral Fellow
Eugene Lifshits, Research Technologist
Hannah Archibald, Research Technician
Hillary Mulvey, Research Technician
Erin Silva, Research Technician
Max Greenberg, Research Technician

Assessment of ABT-263 activity across a cancer cell line collection leads to a potent combination therapy for small-cell lung cancer

Anthony C. Faber[a,b,1,2,3], Anna F. Farago[a,b,c,1], Carlotta Costa[a,b,1], Anahita Dastur[a,b], Maria Gomez-Caraballo[a,b], Rebecca Robbins[c], Bethany L. Wagner[c], William M. Rideout III[c], Charles T. Jakubik[a,b], Jungoh Ham[a,b], Elena J. Edelman[a,b], Hiromichi Ebi[a,b,4], Alan T. Yeo[a,b], Aaron N. Hata[a,b], Youngchul Song[a,b], Neha U. Patel[d], Ryan J. March[a,b], Ah Ting Tam[a,b], Randy J. Milano[a,b], Jessica L. Boisvert[a,b], Mark A. Hicks[d], Sarah Elmiligy[c], Scott E. Malstrom[c], Miguel N. Rivera[a,e], Hisashi Harada[d], Brad E. Windle[d], Sridhar Ramaswamy[a,b], Cyril H. Benes[a,b], Tyler Jacks[c], and Jeffrey A. Engelman[a,b,2]

[a]Massachusetts General Hospital Cancer Center, Boston, MA 02129; [b]Department of Medicine, Harvard Medical School, Boston, MA 02115; [c]David H. Koch Institute for Integrative Cancer Research, Massachusetts Institute of Technology, Cambridge, MA 02138; [d]Philips Institute for Oral Health Research, Virginia Commonwealth University School of Dentistry and Massey Cancer Center, Virginia Commonwealth University, Richmond, VA 23298; and [e]Department of Pathology, Massachusetts General Hospital, Boston, MA 02114

Edited by John D. Minna, University of Texas Southwestern Medical Center, Dallas, TX, and accepted by the Editorial Board January 30, 2015 (received for review July 7, 2014)

BH3 mimetics such as ABT-263 induce apoptosis in a subset of cancer models. However, these drugs have shown limited clinical efficacy as single agents in small-cell lung cancer (SCLC) and other solid tumor malignancies, and rational combination strategies remain underexplored. To develop a novel therapeutic approach, we examined the efficacy of ABT-263 across >500 cancer cell lines, including 311 for which we had matched expression data for select genes. We found that high expression of the proapoptotic gene Bcl2-interacting mediator of cell death (*BIM*) predicts sensitivity to ABT-263. In particular, SCLC cell lines possessed greater BIM transcript levels than most other solid tumors and are among the most sensitive to ABT-263. However, a subset of relatively resistant SCLC cell lines has concomitant high expression of the antiapoptotic myeloid cell leukemia 1 (MCL-1). Whereas ABT-263 released BIM from complexes with BCL-2 and BCL-XL, high expression of MCL-1 sequestered BIM released from BCL-2 and BCL-XL, thereby abrogating apoptosis. We found that SCLCs were sensitized to ABT-263 via TORC1/2 inhibition, which led to reduced MCL-1 protein levels, thereby facilitating BIM-mediated apoptosis. AZD8055 and ABT-263 together induced marked apoptosis in vitro, as well as tumor regressions in multiple SCLC xenograft models. In a *Tp53; Rb1* deletion genetically engineered mouse model of SCLC, the combination of ABT-263 and AZD8055 significantly repressed tumor growth and induced tumor regressions compared with either drug alone. Furthermore, in a SCLC patient-derived xenograft model that was resistant to ABT-263 alone, the addition of AZD8055 induced potent tumor regression. Therefore, addition of a TORC1/2 inhibitor offers a therapeutic strategy to markedly improve ABT-263 activity in SCLC.

small-cell lung cancer | targeted therapies | BH3 mimetics | apoptosis | BIM

Effective cancer-targeted therapies often trigger cell death, commonly via apoptosis, to induce remissions (1–3). For example, we and others previously observed that, among lung cancers with activating *EGFR* mutations, those with higher expression levels of Bcl2-interacting mediator of cell death (BIM), a key regulator of apoptosis, have a higher response rate and longer progression-free survivals upon treatment with EGFR inhibitors (2, 4). BH3 mimetics are a class of drugs designed to promote apoptosis. These compounds bind to and inhibit antiapoptotic BCL-2 family members, the molecular sentinels of apoptosis. ABT-263 (5) is a BH3 mimetic that directly binds BCL-2 and BCL-XL, which blocks their binding to BIM and thereby enables BIM-mediated induction of apoptosis (6–8). However, ABT-263 does not bind the prosurvival BCL-2 family member myeloid cell leukemia 1 (MCL-1), and high levels of MCL-1 are associated with resistance to BH3 mimetics such as ABT-263 in both the laboratory and the clinic (9–17).

Small-cell lung cancer (SCLC) is a high-grade neuroendocrine carcinoma that accounts for 10–15% of all lung cancers and is commonly associated with a significant tobacco history. Patient outcomes have not improved substantially over the past 30 y, underscoring the need for more effective treatment strategies (18). Recent studies have demonstrated the antitumor activity of BH3 mimetics in laboratory models of SCLC (5, 19–21). These findings spurred clinical trials of the BH3 mimetic ABT-263

Significance

Small-cell lung cancer (SCLC) is an aggressive carcinoma with few effective treatment options beyond first-line chemotherapy. BH3 mimetics, such as ABT-263, promote apoptosis in SCLC cell lines, but early phase clinical trials demonstrated no significant clinical benefit. Here, we examine the sensitivity of a large panel of cancer cell lines, including SCLC, to ABT-263 and find that high Bcl2-interacting mediator of cell death (BIM) and low myeloid cell leukemia 1 (MCL-1) expression together predict sensitivity. SCLC cells relatively resistant to ABT-263 are sensitized by TORC1/2 inhibition via MCL-1 reduction. Combination of ABT-263 and TORC1/2 inhibition stabilizes or shrinks tumors in xenograft models, in autochthonous SCLC tumors in a genetically engineered mouse model, and in a patient-derived xenograft SCLC model. Collectively, these data support a compelling new therapeutic strategy for treating SCLC.

Author contributions: A.C.F., A.F.F., C.H.B., T.J., and J.A.E. designed research; A.C.F., A.F.F., C.C., M.G.-C., R.R., B.L.W., W.M.R., C.T.J., J.H., A.T.Y., Y.S., N.U.P., M.A.H., S.E., and S.E.M. performed research; R. J. March, A.T.T., R. J. Milano, J.L.B., and H.H. contributed new reagents/analytic tools; A.C.F., A.F.F., C.C., A.D., M.G.-C., E.J.E., H.E., A.T.Y., A.N.H., M.N.R., B.E.W., S.R., C.H.B., T.J., and J.A.E. analyzed data; and A.C.F., A.F.F., C.H.B., and J.A.E. wrote the paper.

Conflict of interest statement: J.A.E. receives sponsored research from Novartis and AstraZeneca and consults for Novartis and AstraZeneca. H.E. receives sponsored research from AstraZeneca.

This article is a PNAS Direct Submission. J.D.M. is a guest editor invited by the Editorial Board.

[1]A.C.F., A.F.F., and C.C. contributed equally to this work.

[2]To whom correspondence may be addressed. Email: acfaber@vcu.edu or jengelman@partners.org.

[3]Present address: Philips Institute for Oral Health Research, VCU School of Dentistry and Massey Cancer Center, Virginia Commonwealth University, Richmond, VA 23298.

[4]Present address: Cancer Research Institute, Kanazawa University, Kanazawa 920-0934, Japan.

This article contains supporting information online at www.pnas.org/lookup/suppl/doi:10.1073/pnas.1411848112/-/DCSupplemental.

(Navitoclax) in SCLC (22). ABT-263 was well tolerated in the clinic with a dose-limiting toxicity of thrombocytopenia (22), an on-target toxicity of BCL-XL inhibition (23). Unfortunately, phase II trials of ABT-263 monotherapy revealed unimpressive activity. Sixteen of 26 evaluable patients had progression of disease, 9 had stable disease, and one had a partial response (24). Consequentially, there has been no further clinical development of ABT-263 as a monotherapy in SCLC.

Despite these findings, several questions remain: which solid tumor malignancies are most sensitive to single-agent ABT-263, and why is SCLC among the most sensitive? In addition, why does SCLC fail to respond to single-agent ABT-263 in the clinic, and how could efficacy be enhanced? Here, we assess the sensitivity of a large panel of cell lines spanning multiple cancer types to ABT-263. We observe that cell lines with high expression of BIM are highly sensitive to ABT-263 and that SCLC expresses higher levels of BIM than other solid tumor malignancies. Although SCLC is among the most sensitive to single-agent ABT-263, efficacy is substantially limited by MCL-1, which also is elevated in SCLC. We find that SCLC can be sensitized to ABT-263 via TORC1/2 inhibition, which leads to reduction of MCL-1 protein levels, thereby permitting BIM-mediated apoptosis. In two SCLC mouse xenograft models, either drug alone has little activity. However, the combination ABT-263 and AZD8055 induces tumor stabilization or regression. Furthermore, we examined the efficacy of this combination in autochthonous lung tumors arising in a genetically engineered mouse model (GEMM) of SCLC, where the combination of ABT-263 and AZD8055 also induces tumor stabilization or regression. By contrast, most tumors progress when treated with either drug alone. Finally, in a patient-derived xenograft model of SCLC in which ABT-263 alone is ineffective, the combination of ABT-263 and AZD8055 causes tumor regression. These studies demonstrate that the combination of ABT-263 and AZD8055 potently suppresses tumor progression across a variety of preclinical SCLC experimental models.

Results

BIM/MCL-1 Ratio Predicts Sensitivity to ABT-263. Our initial studies stemmed from the observation that 5 of 11 SCLC human xenografts tested by Shoemaker and colleagues (19) did not respond to ABT-263 and that the majority of patients treated in a phase II study had progression of disease (24). To more broadly identify mediators of response to ABT-263, we examined data collected from a high-throughput drug screen (13) assessing over 500 human cancer cell lines for sensitivity to ABT-263. Because the mechanism underlying ABT-263 activity putatively relies on releasing BIM to promote apoptosis (6), we hypothesized that BIM levels may predict responsiveness to ABT-263. By matching cell line sensitivity to two independent gene expression data sets, we found a modest, but significant, correlation between *BIM* expression and sensitivity to ABT-263 (Fig. 1*A* and *SI Appendix*, Fig. S1*A*). As we and others have reported (10, 13–17), high *MCL-1* expression correlated with resistance to ABT-263 and the related ABT-737, and we also observed MCL-1–based resistance to ABT-263 across both data sets (*SI Appendix*, Fig. S1 *B* and *C*). However, the ratio of *BIM* to *MCL-1* predicted sensitivity to ABT-263 more effectively than the expression of either biomarker alone (Fig. 1*B* and *SI Appendix*, Fig. S1*D*). Moreover, among cell lines, those with the highest *BIM* levels that also expressed high levels of *MCL-1* were not sensitive to ABT-263 nor were those cancers with low expression of both *BIM* and *MCL-1*, underscoring the added value of measuring the ratio of *BIM* to *MCL-1* in predicting sensitivity (Fig. 1*C* and *SI Appendix*, Fig. S1*E*). It is notable that the ratio of either *BCL-2* or *BCL-XL* to *MCL-1* was inferior to the ratio of *BIM* to *MCL-1* at predicting response to ABT-263 across solid tumor cancers (*SI Appendix*, Fig. S2). These findings underlie the potential capacity for MCL-1 to mitigate the therapeutic benefit of ABT-263 in cancers with high BIM levels.

We found that SCLC lines have increased BIM expression compared with other solid tumor types (Fig. 1*D* and *SI Appendix*, Fig. S3)

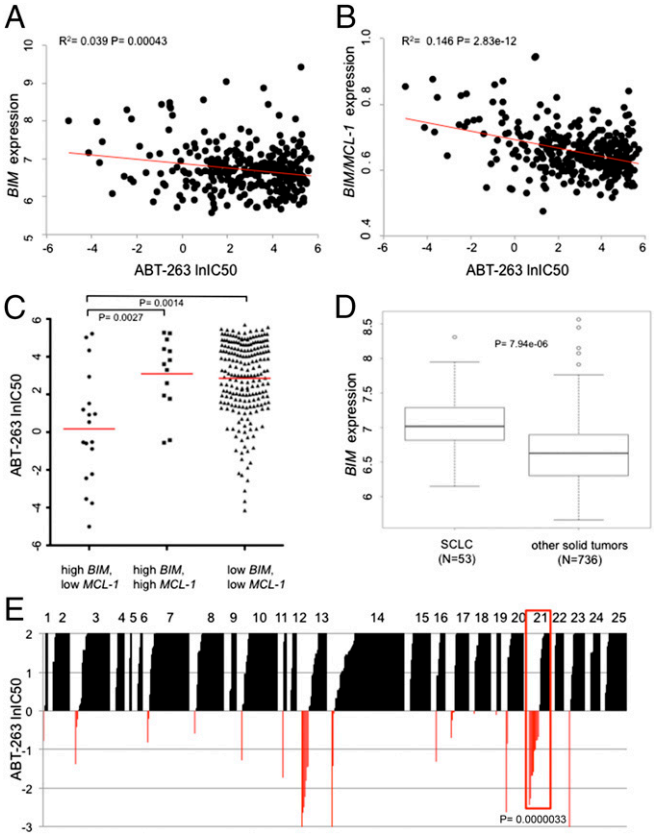

Fig. 1. *BIM/MCL-1* expression ratios predict response to ABT-263. (*A*) Scatter plot of ABT-263 IC_{50} (μM) values on natural log scale versus relative *BIM* RNA expression levels measured from the Cancer Cell Line Encyclopedia (CCLE) (45) (n = 331). A linear regression analysis was used to assign a coefficient of determination (R^2) of 0.039 and a P value of 0.00043. (*B*) Scatter plot of ABT-263 IC_{50} (μM) values on the natural log scale versus the ratio of *BIM*/*MCL-1* expression levels. A linear regression analysis was used to assign a coefficient of determination (R^2) of 0.146 and a P value of 2.83e-12. Expression values were taken from the CCLE (45). (*C*) Scatter plots comparing ABT-263 IC_{50} (μM) values on the natural log scale between cell lines with high BIM expression (top 10%) and low *MCL-1* expression (bottom 75%), cell lines with high BIM expression (top 10%) and high *MCL-1* expression (top 25%), and cell lines with low *BIM* expression and low *MCL-1* expression. Expression values were taken from the CCLE (45). An unpaired t test with Welch's correction was used to assign a P value for differential IC_{50}'s between the *BIM* high/*MCL-1* low group and the two other groups; $P = 0.0027$ and $P = 0.0014$, respectively. Red bars are the geometric means of the IC_{50}'s for the groups of cell lines. (*D*) Box plot showing increased expression of BIM in SCLC cell lines compared with other solid tumors. A Wilcoxon rank-sum test was used to assign a P value for differential expression between the two groups; P value of 7.94e-06. Expression values were taken from the CCLE (45). (*E*) Cancer cell lines were grouped by cancer type, represented by a numeric value, and correlated to ABT-263 IC_{50} (μM) values on natural log scale. The key for the different cancer types is in *SI Appendix*, Fig. S4. A box is drawn around SCLC (#21) for emphasis. Sensitive cell lines were set at IC_{50}'s <1 μM and insensitive cell lines >1 μM. Based on these criteria, a P value of 0.0000033 was assigned from a two-tailed Fisher's exact test comparing SCLC to other solid tumor types. Of note, there were 10 sensitive SCLC cell lines and 11 insensitive SCLC cell lines (48% sensitive). In contrast, among all other solid tumor types, there were 37 sensitive and 443 resistant cancers (8% sensitive). Note that representative cancer types are shown and not every cancer type analyzed is included.

along with enhanced sensitivity to ABT-263 compared with other solid tumor types across a large panel of cancer cell lines (Fig. 1*E* and *SI Appendix*, Fig. S4). To determine whether ABT-263 sensitivity in SCLC was mediated by high *BIM* expression, we knocked down *BIM* using siRNA. Knockdown with two different siRNAs designed against *BIM* in SCLC cell lines consistently suppressed ABT-263–induced apoptosis by >50% (Fig. 2 *A* and *B* and

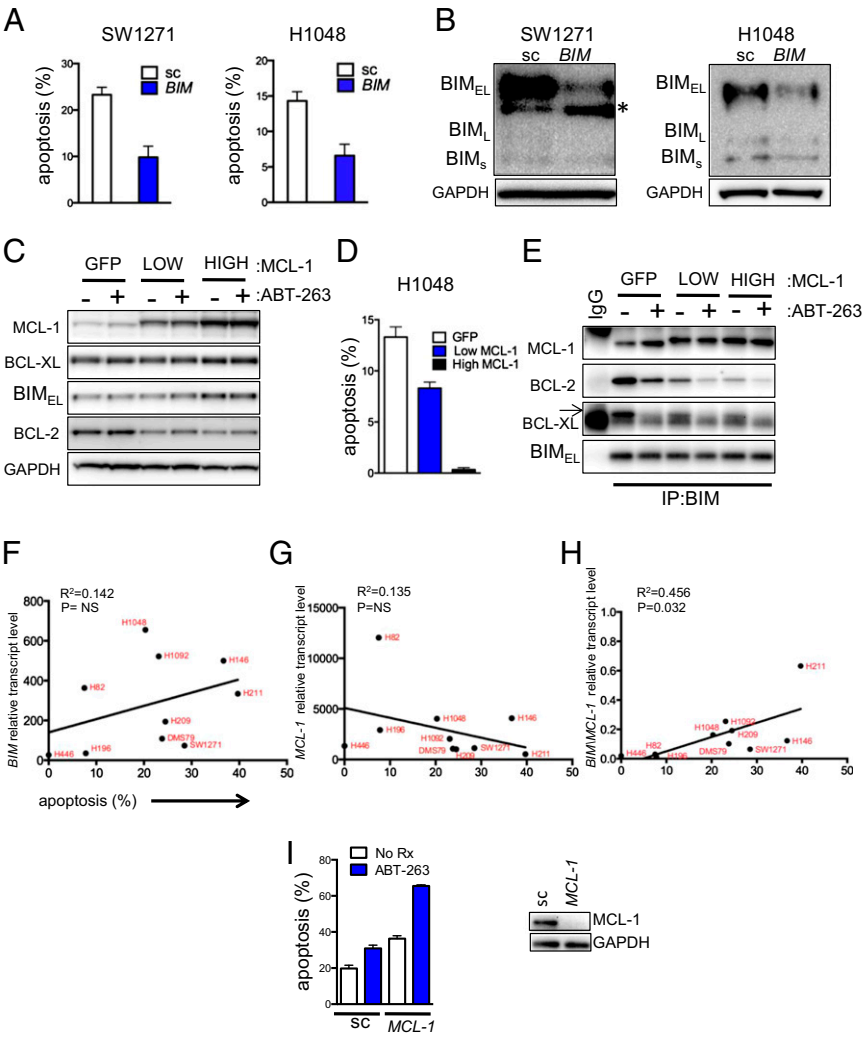

Fig. 2. BIM and MCL-1 mediate ABT-263–induced apoptosis in SCLC, and the ratio of BIM to MCL-1 expression predicts the magnitude of apoptosis in SCLC cell lines. (*A*) SCLC SW1271 and H1048 cells were treated with either 10 nM scrambled (sc) or *BIM* siRNA (2), and, the next day, cells were treated with or without ABT-263. Then, cells were (*A*) prepared and stained with propidium iodide and Annexin-V. Apoptosis was measured by FACS analysis of the percentage of cells positive for Annexin-V 72 h after treatment (the amount of apoptotic cells caused by ABT-263 treatment minus no drug treatment) or (*B*) lysed and separated by SDS/PAGE, subjected to Western blot, and probed with the indicated antibodies. In *A*, error bars are SD ($n = 3$); in *B*, the asterisk indicates a nonspecific band. (*C*) H1048 cells transduced with lentiviral particles containing plasmids that express GFP alone (control) or GFP-IRES-MCL-1. MCL-1–overexpressing cells were sorted to isolate cells expressing low and high amounts of MCL-1 based on GFP fluorescence intensity. Protein lysates were prepared and probed with the indicated antibodies. (*D*) The cells were treated with either no drug (control) or ABT-263 for 48 h. Cells were prepared and stained with propidium iodide and Annexin-V. Apoptosis was measured by FACS analysis of the percentage of cells with Annexin-V positivity. Bars represent mean percentage of apoptotic cells, ABT-263 treatment minus control. Error bars are SD ($n = 3$). (*E*) BIM antibody (or IgG control) was added to lysates following treatment with or without ABT-263 for 6 h derived from H1048 cells expressing GFP, low MCL-1, or high MCL-1 (as in *C*), and BIM-containing complexes were immunoprecipitated and separated by SDS/PAGE, subjected to Western blot, and probed with the indicated antibodies. (*F*) *BIM* RNA levels or (*G*) *MCL-1* RNA levels in a panel of 10 human SCLC cell lines were determined by quantitative PCR, and the average of three replicates was plotted versus the amount of apoptosis ($n = 3$) induced by 1 μM of ABT-263 over 72 h. Each dot represents a unique human SCLC line labeled in red font, with RNA levels relative to *GAPDH* abundance. A linear regression analysis was used to assign, for *F*, a coefficient of determination (R^2) of 0.142 and a *P* value of 0.284 (*P* = not significant), and for *G*, a coefficient of determination (R^2) of 0.135 and a *P* value of 0.296 (*P* = not significant). (*H*) *BIM*/*MCL-1* RNA levels were plotted versus apoptosis in the same lines. A linear regression analysis was used to assign a coefficient of determination (R^2) of 0.456 and a *P* value of 0.032. (*I*) SCLC H1048 cells were treated with either 50 nM scrambled (sc) or *MCL-1* siRNA for 24 h. Cells were reseeded and treated the following day with no drug (control) or ABT-263 and then prepared for FACS analysis of percentage of cells with Annexin-V positivity 24 h after treatment. Error bars are SD ($n = 3$). (*Right*) Cell lysates were prepared from the transfected cells and separated by SDS/PAGE, subjected to Western blot, and probed with the indicated antibodies.

SI Appendix, Fig. S5 *A* and *B*). Next, we engineered H1048 SCLC cells to have either modest ("low") or marked ("high") overexpression of MCL-1 (Fig. 2*C* and *SI Appendix*, Fig. S5*C*). Increasing expression of MCL-1 protected cells from ABT-263–induced apoptosis (Fig. 2*D*). These results support the model that high BIM and low MCL-1 promote sensitivity to ABT-263, whereas high MCL-1 mediates ABT-263 resistance.

To further assess the mechanism of ABT-263 response, we performed immunoprecipitation of BIM complexes from whole-cell lysates. Please note that the BIM immunoprecipitations successfully depleted >90% of the cellular BIM (*SI Appendix*, Fig. S5*D*). In control cells, ABT-263 treatment led to loss of BIM binding to BCL-XL and BCL-2, whereas it induced BIM binding to MCL-1 (Fig. 2*E*). This indicates that MCL-1 binds the BIM that is

released from complexes with BCL-2 and BCL-XL upon treatment with ABT-263. This likely contributes to the mechanism whereby MCL-1 expression mitigates the apoptotic response induced by ABT-263. Incremental overexpression of MCL-1 resulted in more BIM/MCL-1 complexes (Fig. 2*E*) and fewer BIM/BCL-2 complexes, consistent with the abrogation of apoptosis induced by MCL-1 overexpression. Consistent with these results and similar to the analyses of the large cell line panel described above, BIM or MCL-1 expression alone was not significantly predictive of apoptosis following ABT-263 therapy in a subset of SCLC cell lines (Fig. 2 *F* and *G*). However, the ratio of BIM/MCL-1 correlated significantly with apoptotic response in SCLC cell lines (Fig. 2*H*). Thus, BIM and MCL-1 levels substantially impact sensitivity to ABT-263–mediated apoptosis in SCLC cell lines, with high BIM and low MCL-1 expression associated with enhanced sensitivity to ABT-263.

TORC1/2 Inhibition Suppresses MCL-1 and Sensitizes SCLC Cells to ABT-263. Despite some of the preclinical promise of ABT-263 against SCLC (Fig. 1*E*) (5, 19), ABT-263 has demonstrated minimal clinical activity in SCLC as monotherapy (22, 24). BIM levels are higher in SCLC relative to other solid tumor cell lines (Fig. 1*D* and *SI Appendix*, Fig. S3), but MCL-1 levels are also relatively high in SCLC (*SI Appendix*, Fig. S5*E*), suggesting that high MCL-1 levels may be mitigating the efficacy of ABT-263 in SCLC. Consistent with this notion, knockdown of MCL-1 using two different siRNAs sensitized the H1048 SCLC cell line to ABT-263 (Fig. 2*I* and *SI Appendix*, Fig. S6*A*). We therefore sought to identify pharmacological strategies that could suppress MCL-1 levels and increase sensitivity to ABT-263. We did not pursue obatoclax, which does target MCL-1 in addition to other BCL-2 family members, because early clinical trials suggest that obatoclax causes toxicity independent of its effects on BCL-2 family proteins, potentially limiting its clinical utility (25–27). Rather, we considered TORC1/2 inhibitors because they suppress MCL-1 protein levels in some cancers (7, 28–31). We observed that the TORC1/2 catalytic inhibitor AZD8055 (32) potently suppressed protein levels of MCL-1 in SCLC cells (Fig. 3*A*) and markedly enhanced ABT-263–induced apoptosis in four different SCLC cell lines examined (Fig. 3*B*). BIM immunoprecipitations confirmed that AZD8055 abrogated the formation of MCL-1/BIM complexes normally induced by ABT-263 treatment (Fig. 3*C* and *SI Appendix*, Fig. S6*B*; compare the combination to ABT-263). Consistent with the proposed mechanism of apoptosis induced by this combination, overexpression of MCL-1 blocked apoptosis induced by the combination (Fig. 3*D* and *SI Appendix*, Fig. S6 *C* and *D*). Importantly, AZD8055 and ABT-263 interfered with cell cycle progression in all SCLC cell lines (*SI Appendix*, Fig. S7). Thus, the combination of ABT-263 and AZD8055 both increased apoptosis and induced growth arrest of SCLCs, suggesting that this combination could be of superior efficacy compared with treatment uniquely targeting BCL-2 family members. Interestingly, we found that treatment of SCLC cells with rapamycin, an allosteric mTOR inhibitor, diminished expression of pS6, a downstream target of TORC1, but, unlike AZD8055 therapy, failed to suppress p4E-BP1 signaling, lower MCL-1 levels, or sensitize to ABT-263 as well as AZD8055 (*SI Appendix*, Fig. S8 *A* and *B*). These data are consistent with other studies demonstrating that TORC1/2 catalytic inhibitors more effectively suppress 4E-BP1 phosphorylation and cap-dependent translation than rapamycin or rapalogs (31, 33). In fact, resistance to single-agent AZD8055 has been reported to emerge through reactivation of cap-dependent translation, including that of MCL-1, in the presence of the drug (34). Of note, although others found that BCL2-associated X protein (BAX) plays a role in rapamycin sensitization of ABT-737 (35), we did not observe an increase in BAX expression in the ABT-263/AZD8055 combination treatment compared with ABT-263 treatment (*SI Appendix*, Fig. S8*C*) despite the induction of substantial apoptosis (~20%) at the same time point (*SI Appendix*, Fig. S8*D*).

Previous studies have suggested that mTOR is necessary for efficient cap-dependent translation of MCL-1, and thus mTOR inhibitors may decrease MCL-1 expression by decreasing translation. To determine if AZD8055 affected the half-life of MCL-1 protein, we treated H1048 cells with the cytoplasmic protein synthesis inhibitor, cycloheximide (CHX), alone or in combination with AZD8055. We found the rate of MCL-1 protein degradation was comparable over time in the CHX-treated cells versus the CHX+AZD8055 combination-treated cells, suggesting a similar mode of MCL-1 inhibition between CHX and AZD8055 (*SI Appendix*, Fig. S9*A*). Treatment at 6 h with AZD8055 alone left a nearly equivalent amount of cellular MCL-1 as CHX alone or the combination of CHX and AZD8055 (*SI Appendix*, Fig. S9 *A* and *B*). These data are consistent with translational inhibition being the major mechanism underlying suppression of MCL-1 protein levels following mTORC inhibition.

Combination of ABT-263 and AZD8055 Causes Tumor Regression in Xenograft Models. We next assessed the efficacy of AZD8055 and ABT-263 in vivo using H1048 and H82 SCLC cell line xenograft tumor models. ABT-263 has been shown to be only modestly effective in the H1048 model and minimally effective in the H82 model (19) and therefore may be more representative of SCLC clinical outcomes with single-agent BH3 mimetics such as ABT-263 (22, 24). Consistent with previous data (19), ABT-263 (80 mg/kg/qd) was partially effective in established H1048 xenografts, whereas single-agent AZD8055 (16 mg/kg/qd) modestly slowed tumor growth (Fig. 3*E*). However, the combination induced marked tumor regressions to nearly undetectable sizes (Fig. 3*E*). In the faster-growing H82 xenografts, ABT-263 was ineffective as previously reported (19). Single-agent AZD8055 had a modest effect on tumor growth (Fig. 3*E*). However, the combination almost completely blocked growth of these tumors (Fig. 3*E*). Pharmacodynamic studies confirmed that AZD8055 suppressed phosphorylation of TORC1 targets S6 and 4E-BP1 and decreased MCL-1 protein levels in vivo (Fig. 3*F*). Moreover, cleaved caspase 3, a marker of apoptosis, was significantly increased following combination treatment (Fig. 3*G* and *SI Appendix*, Fig. S10*A*), consistent with the in vitro studies. No overt toxicities were observed in the tumor bearing mice treated with the combination (*SI Appendix*, Fig. S10*B*).

Combination of ABT-263 and AZD8055 Is Superior to Either Drug Alone in a SCLC Genetically Engineered Mouse Model. Although cell line xenograft models of SCLC are valuable tools for assessing drug activity in vivo, they may not fully model the tissue environment and heterogeneity of autochthonous tumors (those growing in their native tissue context). To rigorously assess the activity of the combination of ABT-263 and AZD8055 in vivo, we used a GEMM of SCLC (36). Tumors are initiated in this model via conditional inactivation of both alleles of *Tp53* and *Rb1* in pulmonary neuroendocrine cells, resulting in the development of tumors that model the histology, metastatic spread, and acquired genetic alterations observed in human SCLC (37–39). Tumor-bearing SCLC GEMMs were randomized to receive no treatment, AZD8055 alone (16mg/kg/qd), ABT-263 alone (80 mg/kg/qd), or both ABT-263 and AZD8055 and were treated for 21 d (Fig. 4*A*). Magnetic resonance imaging (MRI) of the thorax was performed 1 day before starting treatment and on day 21 of treatment, and lung tumor volumes pre- and posttreatment were quantified. Most animals had exactly one measurable lung tumor. If more than one tumor was observed in separate lobes of the lungs, the larger tumor was measured. Only tumors that were histologically confirmed to be high-grade neuroendocrine tumors or had clear evidence of distant metastatic spread on MRI were included in the analysis. Tumors progressed in all untreated animals ($n = 7$), although we observed significant variability in the rate of progression over the 21-d period (Fig. 4 *B–D*

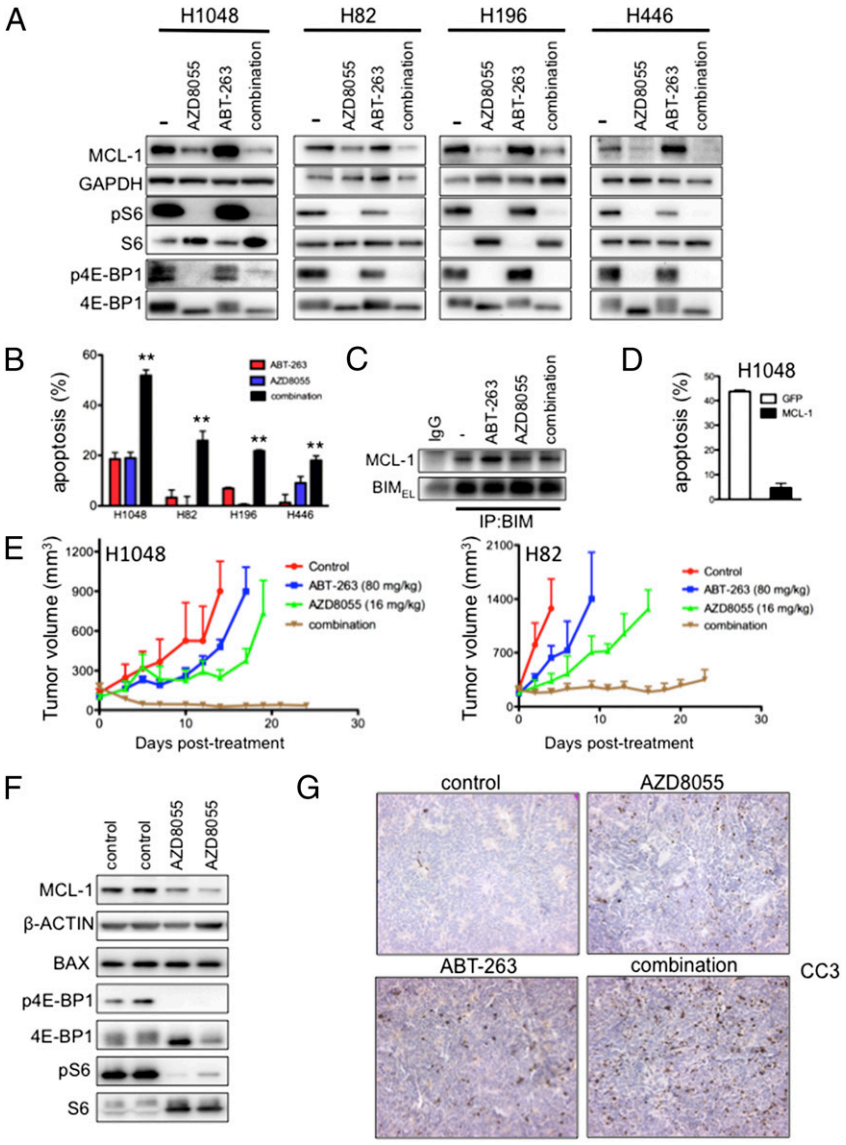

Fig. 3. Combination treatment with ABT-263 and the TORC1/2 inhibitor AZD8055 leads to robust apoptosis and antitumor activity in vivo. (*A* and *B*) The indicated SCLC cell lines were treated with no drug (–), 500 nM AZD8055, 1 μM ABT-263, or a combination of 500 nM AZD8055 and 1 μM ABT-263. (*A*) After 16 h of treatment, lysates were probed with the indicated antibodies. (*B*) After 72 h of treatment, cells were prepared and stained with propidium iodide and Annexin-V, and apoptosis was measured by FACS analysis of the percentage of cells with Annexin-V positivity. Bars represent mean the amount of apoptosis induced by each treatment minus control. Error bars are SD ($n = 3$). $^{**}P < 0.05$ by Student's *t* test, ABT-263 versus combination treatment group and AZD8055 versus combination group. (*C*) H1048 cells were treated with no drug (–), 1 μM ABT-263, 500 nM AZD8055, or 500 nM AZD8055/1 μM ABT-263 for 2 h, and lysates were immunoprecipitated with BIM antibody or IgG negative control. Precipitates were analyzed by Western blot analyses with the indicated antibodies. (*D*) H1048 cells transduced with lentiviral particles expressing GFP alone (GFP) or GFP-IRES-MCL-1 (the "high"-expressing MCL-1 cells from Fig. 2*C*) were treated with either no drug (–) or 500 nM AZD8055/1 μM ABT-263. Following 72 h of treatment, cells were prepared and stained with propidium iodide and Annexin-V, and apoptosis was measured by FACS analysis of the percentage of cells with Annexin-V positivity. Bars represent mean percentage of apoptotic cells following combination treatment over control. Error bars are SD ($n = 3$). (*E*) Human SCLC H1048 and H82 cells were grown as xenograft tumors in Nu/Nu mice, and, when tumors were ~100–200 mm^3, mice were randomized into treatment cohorts: control (no drug), 16 mg/kg/qd AZD8055, 80 mg/kg/qd ABT-263, or the combination of AZD8055 and ABT-263. AZD8055 was given ~1.5 h before ABT-263 for combination treatments. Tumor measurements were performed approximately three times per week by calipers, and the average tumor volume + SEM for each cohort is displayed. (*F*) Tumors were harvested from H1048 tumor-bearing mice approximately 3 h after drug administration at the end of treatment and tumor lysates were subjected to Western blot analyses and probed with the indicated antibodies. (*G*) Slides were prepared from formalin-fixed tissue of H1048-tumor bearing mice approximately 3 h after drug administration and stained with CC3 to quantify apoptosis. Quantification of CC3 is shown in *SI Appendix*, Fig. S10*A*.

and *SI Appendix*, Table S1). All tumors treated with AZD8055 alone progressed ($n = 5$) (Fig. 4 *B*, *E*, and *F* and *SI Appendix*, Table S1). Of six tumors treated with ABT-263, five progressed and one regressed (Fig. 4 *B*, *G*, and *H* and *SI Appendix*, Table S1). By contrast, in six animals treated with the combination of ABT-263 and AZD8055, three tumors regressed and three others showed relatively limited tumor progression (Fig. 4 *B*, *I*, and *J* and *SI Appendix*, Table S1). The responses of tumors to the combination of ABT-263 and AZD8055 were significantly superior to responses either to the drug alone or to no treatment. Consistent with these findings and those in the human xenograft models (Fig. 3 *E*–*G*), CC3 staining in allografted SCLC GEMM tumors was markedly apparent in the combination treatment at the 3-d time point (Fig. 4 *K*–*N*), again indicating a strong apoptotic response following administration of this regimen. Ex vivo cell lines derived from SCLC GEMMs treated with AZD8055 had reduction of MCL-1 protein levels and were sensitized

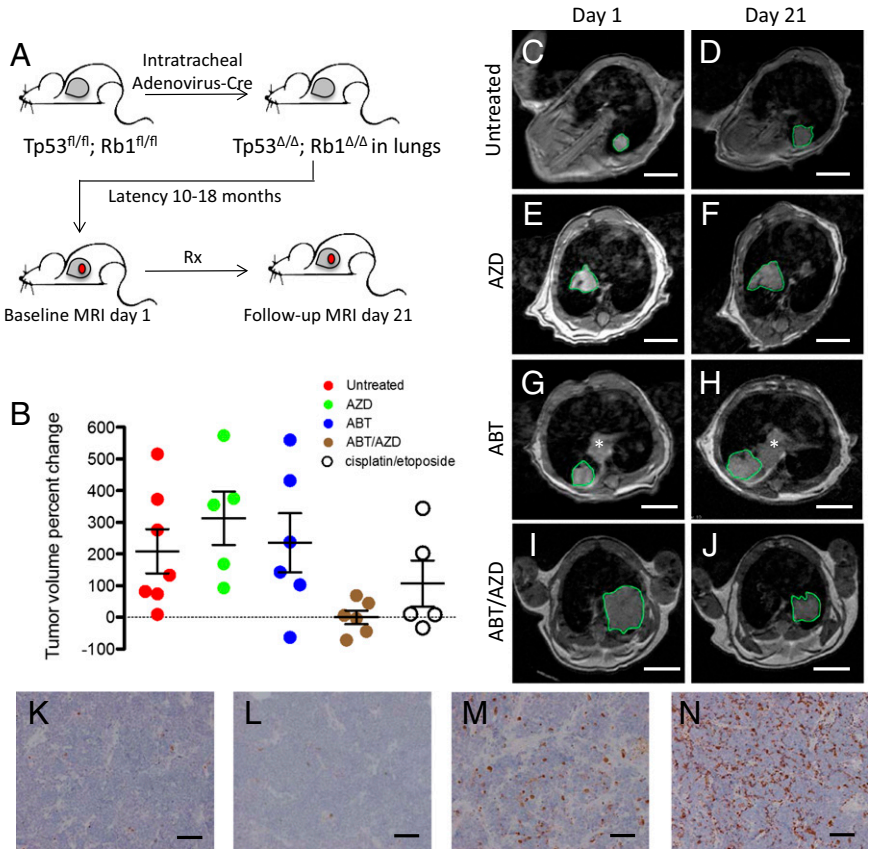

Fig. 4. Combination ABT-263 and AZD8055 induce tumor regressions in a GEMM of SCLC. (*A*) Schematic of GEMM experiment. Gray space in mouse drawing indicates lung; red circle indicates lung tumor. (*B*) SCLC GEMMs harboring radiographically measurable lung tumors were randomized to receive treatment for 21 d with 80 mg/kg/day ABT-263, 16 mg/kg/day AZD8055, combination ABT-263/AZD8055, or no treatment. Chest and upper abdomen were imaged by MRI on the day before starting treatment and on day 21 of treatment. For each animal, the largest single lung tumor that was histologically confirmed to be a high-grade neuroendocrine tumor was measured radiographically, and volume was computed. The percentage of tumor volume change for each animal is plotted as a single circle, with black bars indicating mean and SEM. Also included for comparison is the percentage of tumor volume change by MRI when equivalent GEMMs were treated with cisplatin (7 mg/kg IP on days 1 and 8) and etoposide (10 mg/kg on days 2 and 9). Notably, the follow-up imaging time point for the chemotherapy-treated animals was 28 d. Unpaired two-tailed *t* tests for statistical significance comparing tumor volume percentage change between pairs of datasets were performed. Untreated versus ABT-263/AZD8055: $P = 0.0222$. AZD8055 versus ABT-263/AZD8055: $P = 0.00350$. ABT-263 versus ABT-263/AZD8055: $P = 0.0333$. Cisplatin/etoposide versus ABT-263/AZD8055: 0.1589 (not significant). (*C–J*) Representative examples of MRI images (with tumors outlined in green) on day 1 and day 21 of a 21-d treatment period, with the treatment indicated. The asterisk in *G* and *H* indicates additional tumor in a separate lobe, which is not included in measurements. (Scale bar: 5.0 mm.) (*K–N*) A GEMM SCLC tumor was dissected from the lung and implanted s.c. into a NSG mouse. An established tumor in the NSG mouse was then divided and s.c. implanted directly into four nu/nu NSG mice. There was no in vitro intermediate. Once tumors were established, nu/nu mice were treated for 3 d with (*K*) vehicle for both drugs, (*L*) AZD8055 (16 mg/kg/qd), (*M*) ABT-263 (80 mg/kg/qd), (*N*) ABT-263 (80 mg/kg PO daily), and AZD8055 (16 mg/kg PO daily). Tumors were collected and fixed 3 h after the final treatment. Sections from tumor were stained to detect CC3, shown as brown stain. (Scale bar: 100 μm.)

to ABT-263 (*SI Appendix*, Fig. S11 *A* and *B*), consistent with the mechanism delineated in human cell lines and the activity observed in vivo.

SCLC tumors often respond to first-line chemotherapy in patients, although these responses are almost invariably transient. To provide context for the responsiveness to the AZD8055/ABT-263 combination in the SCLC GEMM model, we treated mice with a combination of cisplatin (7 mg/kg IP on days 1 and 8) and etoposide (10 mg/kg on days 2 and 9), the standard chemotherapies used to treat SCLC in patients. When we compared responses to the combination chemotherapy at day 28 to responses to the targeted therapy combination at day 21, the regimen of ABT-263 and AZD8055 improved responses, although the differences did not reach statistical significance (Fig. 4*B*). These data show an encouraging efficacy of the ABT-263/AZD8055 combination therapy in reference to standard of care chemotherapy in this model.

AZD8055 Sensitizes a SCLC Patient-Derived Xenograft Model to ABT-263. To further gain insight into the translational potential of our findings, we next determined the efficacy of the combination in a third type of in vivo model, a patient-derived xenograft (PDX). This type of in vivo model may more faithfully recapitulate the high degree of genomic complexity of the human disease. Patient-derived xenografts derived from a histologically confirmed SCLC case were implanted into NOD *scid* gamma (NSG) mice, and mice were monitored for tumor growth (Fig. 5*A* and *SI Appendix*, Fig. S12). Growing tumors were subsequently treated with either single-agent ABT-263 (80 mg/kg/qd) ($n = 4$) or the combination of ABT-263 (80 mg/kg/qd) and AZD8055 (16 mg/kg/qd) ($n = 4$) (there were not enough tumor-bearing mice to treat with single-agent AZD8055). Consistent with a recent report highlighting overall modest activity of ABT-737 against PDXs of SCLC (35), the tumors in all mice treated with single-agent ABT-263 grew fairly rapidly despite drug treatment (Fig. 5*A*). In contrast, the addition of AZD8055 to ABT-263 led to consistent tumor regressions and showed no sign of regrowth when the experiment was ended ~50 d after drug treatments began (Fig. 5*A*). Additionally, pharmacodynamic analyses of the tumors demonstrated marked decrease in MCL-1 expression in the combination cohort (Fig. 5*B*).

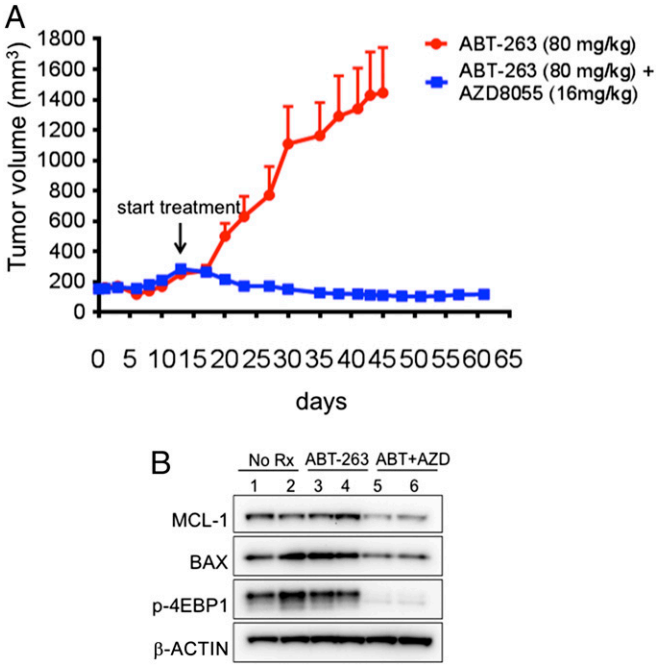

Fig. 5. Addition of AZD8055 to ABT-263 sensitizes a PDX model of SCLC. (*A*) Pieces of a patient-derived SCLC tumor were implanted into NSG mice and monitored for subsequent growth. Upon growing to ~150–300 mm^3, tumors were treated with ABT-263 (80 mg/kg/qd) or ABT-263 (80 mg/kg/qd) plus AZD8055 (16 mg/kg/qd). AZD8055 was given ~1.5 h before ABT-263 for combination treatments. Tumor measurements were performed approximately three times per week by calipers, and the average tumor volume + SEM for each cohort is displayed. Treatment start is indicated by an arrow. (*B*) Approximately 3 h after final drug administration, tumors were surgically excised and tumor lysates were prepared and subjected to Western blot analyses and probed with the indicated antibodies. ABT-263–treated and ABT-263 and AZD8055 combination–treated (ABT+AZD) tumors were compared to two untreated tumors (No Rx). Each number represents a tumor from a unique mouse.

These data indicate substantial activity of this combination in a third type of SCLC preclinical model and demonstrate that, in a SCLC PDX model, AZD8055 down-regulates MCL-1 to sensitize SCLC to ABT-263.

Efficacy of Low-Dose ABT-263 Plus AZD8055 in Vitro and in Vivo. Therapeutic dosing in humans is sometimes limited by drug toxicities that often preclude sufficient target inhibition in patients. The synergistic effect of the ABT-263/AZD8055 combination prompted us to test whether lower doses of either AZD8055 or ABT-263 could still efficiently suppress cell viability and demonstrate in vivo efficacy. In human SCLC cell lines, we found that even low-nanomolar doses of AZD8055 (5 or 16.66 nM) were sufficient to sensitize SCLCs to ABT-263 (100 nM) (Fig. 6*A*). This sensitization to low-dose AZD8055 was also observed in the ex vivo cell lines derived from SCLC GEMMs (*SI Appendix*, Fig. S11*B*). Similarly, a low dose of ABT-263 (3.3 nM) was sufficient to strongly suppress cell viability in combination with 50 nM AZD8055 (*SI Appendix*, Fig. S13). In the H211 cell line, which is sensitive to single-agent ABT-263 in vitro and in vivo (19), addition of AZD8055 further sensitized cells to ABT-263 (Fig. 6*A*). Furthermore, in the presence of ABT-263, p4E-BP1 was almost fully suppressed and MCL-1 was significantly down-regulated by low-nanomolar doses of AZD8055 (Fig. 6*B*). In the dose–response analyses, the amount of apoptosis induced by the combination was inversely related with the amount of MCL-1 protein remaining in response to increasing doses of AZD8055 (Fig. 6*C*). These in vitro findings prompted us to assess lower doses of AZD8055 in vivo. Strikingly, a low dose of 2 mg/kg of AZD8055 (Fig. 6*D*, compared with 16 mg/kg, Fig. 3*E*) in combination with ABT-263 (80 mg/kg) was sufficient to induce regressions in the H1048 SCLC xenograft model.

Discussion

Direct targeting of apoptotic regulators has emerged as an effective therapeutic approach in cancer. One such class of compounds includes BH3 mimetics, such as ABT-263, which block the binding of BCL-2 and BCL-XL to BIM and other proapoptotic proteins. In this study, we examined the efficacy of ABT-263 across a panel of cancer cell lines and observed that the ratio of BIM to MCL-1 predicted sensitivity (Fig. 1 and *SI Appendix*, Fig. S1). These data agree with a recent report by Roberts et al. showing that a high BIM to MCL-1 ratio indicated a favorable response to ABT-263 in nine patients with chronic lymphocytic leukemia (11).

There is significant interest in further developing BH3 mimetics to treat SCLC, and thus we specifically sought to improve the efficacy of ABT-263 in these cancers. We found that, although levels of BIM were relatively high in SCLC lines (Fig. 1*D*), MCL-1 levels were also relatively high, contributing to ABT-263 resistance (*SI Appendix*, Fig. S5*E*). Thus, high BIM levels may "prime" SCLC for apoptosis and in this way contribute to the sensitivity of SCLC to ABT-263. However, the lack of sensitivity of SCLC to ABT-263 in the clinic may be a result of high MCL-1 levels in these cancers. Therefore, we used these data as a rationale to develop a novel targeted therapy for SCLC based on the intrinsic high levels of BIM and the need to suppress MCL-1 (via TORC inhibition) to sensitize to ABT-263. The ABT-263/TORC1/2 inhibitor combination strategy was more effective than either agent alone, not only in increasing the induction of apoptosis, but also in suppressing proliferation. Inducing both apoptosis and growth arrest recapitulates the effects of other successful targeted therapy paradigms (2), including EGFR inhibitors for *EGFR* mutant lung cancers and ALK inhibitors for *ALK*-positive lung cancers.

Notably, the enhanced induction of apoptosis and tumor regression by the combination of ABT-263 and AZD8055 was achieved even with low concentrations of AZD8055 in both cell lines and mouse xenografts and was directly correlated with the relative reduction in MCL-1 protein level (Fig. 6). This suggests that AZD8055 may be effectively combined with ABT-263 even at doses that would otherwise be subtherapeutic as a single agent, widening the potential therapeutic window of this combination. As other BH3 mimetics are being currently developed in the clinic, it will be interesting to determine the differential activity of each to build on the promising concept of combining TORC inhibitors with BH3 mimetics.

A recent report by Gardner et al. demonstrated that rapamycin sensitized several SCLC human cell lines and PDXs to the structurally related BH3-mimetic ABT-737 (35). However, our study reveals significant differences between the two approaches. Unlike the TORC catalytic site inhibitor, rapamycin fails to significantly down-regulate MCL-1 (*SI Appendix*, Fig. S8*A*). This finding is consistent with results demonstrating that TORC1/2 catalytic inhibitors more effectively suppress 4E-BP1 phosphorylation and cap-dependent translation than rapamycin or rapalogs (31, 33). Thus, the TORC catalytic inhibitor is uniquely capable of down-regulating MCL-1 protein expression, which is key for the combination to induce apoptosis. Indeed, we found that addition of rapamycin did not consistently increase the amount of apoptosis induced by ABT-263 (*SI Appendix*, Fig. S8*B*). Another major difference between these therapeutic approaches is that the AZD8055/ABT-263 combination appears effective in low-BCL-2–expressing SCLCs (NCI-H82 and NCI-H446, Figs. 3 *B* and *E* and 6*A*), which Gardner et al. (35) found were resistant to the combination of rapamycin with ABT-737. In contrast to the findings reported by Gardner et al. (35), we did not observe that ABT-263, rapamycin, or AZD8055 consistently affected BAX levels (Figs. 3*F* and 5*B* and *SI Appendix*, Fig. S8*C*). One

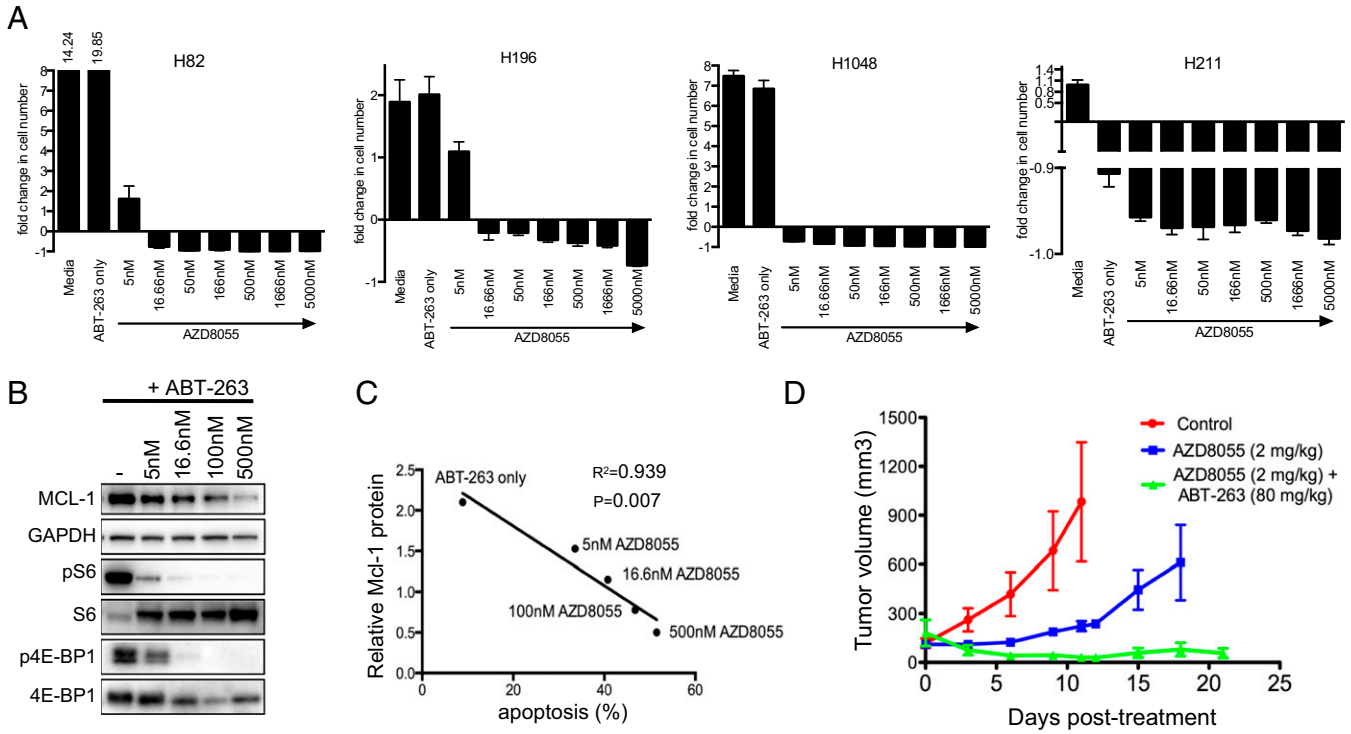

Fig. 6. Low doses of AZD8055 sensitize SCLC to ABT-263. (*A*) SCLC cell lines were treated with no drug (Media), 100 nM ABT-263 (ABT-263 only), or 100 nM ABT-263 in combination with the indicated dose of AZD8055 (ranging from 5 to 5,000 nM AZD8055) for 7 d. The number of viable cells was determined by CellTiter-Glo and presented as fold-change of cells compared with day 0 (i.e., negative values represent loss of cells from day 0). Error bars are SD of cells treated in triplicate. (*B*) H1048 cells were treated with the indicated dose of AZD8055 with 100 nM ABT-263 or 100 nM ABT-263 alone (–) for 16 h, and equal amounts of lysates were subjected to Western blot analyses and probed with the indicated antibodies. (*C*) The amount of MCL-1 protein relative to GAPDH as determined by quantification on a SynGene GBox was plotted against the amount of apoptosis induced by the corresponding 72 h drug treatments (as determined by FACS analysis of the percentage of Annexin-V–positive cells, treatment minus no-treatment control). Note: AZD8055 treatments were in the presence of 100 nM ABT-263, as in (*B*). For the linear regression analysis, the R^2 value was 0.939 and the *P* value was 0.007. (*D*) H1048 cells were grown as xenograft tumors in Nu/Nu mice. When tumors reached ~100–200 mm^3, mice were randomized into treatment cohorts: control (no drug), 2 mg/kg AZD8055, or the combination of AZD8055 (2 mg/kg) and ABT-263 (80 mg/kg). AZD8055 was given ~1.5 h before ABT-263 for combination treatments. Tumor measurements were performed approximately three times per week by calipers, and the average tumor volume ± SEM for each cohort is displayed.

possibility for this difference is that Gardner et al. (35) assessed for changes in BAX expression after more prolonged treatment (1 d to 1 w). Although we did not detect BAX changes after >14 d of treatments in the H1048 xenograft model (Fig. 3*F*) or in the PDX model of SCLC (~50 d of treatment), we assayed for BAX expression only at shorter time points in vitro (16 h). Thus, BAX regulation through TORC1 inhibition may be a later event in some models of SCLC. Importantly, Gardner et al. (35) observed that the mTOR pathway was active in all of the PDX models that they studied, further supporting the concept that combining mTORC catalytic site inhibitors with BH3 mimetics in SCLC could be beneficial.

Interestingly, we observed that the BIM to MCL-1 ratio predicted sensitivity to ABT-263 not only in SCLC, but also across a large panel of cancer cells encompassing a wide range of malignancies (Fig. 1*B* and *SI Appendix*, Fig. S1*D*). We indeed recently reported that combination ABT-263 and AZD8055 also showed efficacy in *KRAS* and *BRAF* mutant colorectal cancers (7). In that study, we demonstrated that AZD8055 led to loss of MCL-1 in those cancers, thereby sensitizing to ABT-263. However, this combination therapy was not effective in *KRAS* and *BRAF* wild-type colorectal cancers, where TORC1/2 inhibition failed to suppress MCL-1. Thus, it is likely that this combination therapy may specifically be effective for cancers in which TORC1/2 inhibition suppresses MCL-1 expression.

We extended our study beyond the more traditional preclinical strategies by using both a SCLC GEMM model and a PDX from a patient with SCLC. Importantly, each autochthonous tumor in the SCLC GEMM model, although initiated by inactivation of *Tp53* and *Rb1*, develops a unique set of additional genetic alterations (39). Furthermore, tumors themselves are heterogeneous, harboring multiple distinct subclones (39). Autochthonous GEMM tumors may therefore more closely recapitulate the genetic heterogeneity found in human SCLC tumors (24, 40, 41) and may be a more rigorous assay for therapeutic efficacy than in vitro studies or mouse xenograft models. They also model the tumor microenvironmental features and immune interactions of human disease more fully than s.c. xenografts in immune-compromised hosts. The fact that we consistently observed stabilization or regression of tumors in response to combination of ABT-263 and AZD8055 in the GEMM, compared with either drug alone, further supports the notion that this combination may be more broadly active in patients than ABT-263 monotherapy. Notably, of six autochthonous tumors treated with ABT-263 alone, one showed significant regression whereas the other five significantly progressed. This range of sensitivities also mirrors the range of sensitivities to ABT-263 in human cell lines and in patients (19, 24).

There was a trend toward GEMM tumors responding more to ABT-263 and AZD8055 than to the standard of care chemotherapies used in patients, cisplatin and etoposide. The relative lack of response of the GEMM tumors to cisplatin and etoposide is interesting because, by contrast, human SCLC tumors have a response rate of ~50% to combination platinum and etoposide (42). Consistent with our findings, Singh and colleagues (43) showed that *Tp53*/*Rb1*-deleted SCLC GEMMs were only modestly sensitive to combination carboplatin and irinotecan, which have similar clinical efficacy as cisplatin and etoposide in patients (42, 44). The SCLC GEMM may therefore more closely resemble a chemotherapy-resistant subset of human SCLC. If this is true, then our

study supports the use of the combination of ABT-263 and TORC1/2 inhibition even in second line setting in patients. Alternatively, it is possible that we did not achieve sufficient levels of cisplatin and etoposide in the mice to induce the extent of tumor regression often seen in patients.

Our PDX study demonstrated lack of efficacy of single-agent ABT-263, consistent with the lack of efficacy observed with single-agent ABT-737 by Gardner et al. (35). The combination, however, induced regressions of all of the combination-treated tumors (Fig. 5*A*). Taken together with the potent efficacy demonstrated in the human xenograft mouse models of SCLC (Fig. 3) and the GEMM model (Fig. 4), the effect of the combination of AZD8055 and ABT-263 was consistent and profound across several mouse models, even at low concentrations of AZD8055 (Fig. 6*D*).

Overall, we found that high BIM levels helped promote sensitivity to BCL-2/BCL-XL inhibitors in SCLC, but efficacy was mitigated by MCL-1. The addition of TORC1/2 inhibitors to BCL-2/BCL-XL inhibitors in SCLCs can lead to marked tumor responses in an array of complementary mouse models and therefore may improve the efficacy of BH3 mimetics for the treatment of SCLC.

Materials and Methods

All materials and methods are described in *SI Appendix*. These include information on cell lines, Western blotting, immunoprecipitation, plasmid preparation, siRNA transfections and shRNA transductions, viability assays, FACS death and cell cycle assays, mouse experiments, and statistical methods.

All studies in GEMM and allograft models were performed under an Institutional Animal Care and Use Committee- and Massachusetts Institute of Technology Committee on Animal Care-approved animal protocol.

The mouse xenografts and patient-derived xenografts were performed in accordance with the Massachusetts General Hospital Subcommittee on Research Animal Care.

ACKNOWLEDGMENTS. We thank the Koch Institute Swanson Biotechnology Center for technical support, specifically the Hope Babette Tang (1983) Histology Facility and the Applied Therapeutics and Live Animal Imaging facility, and Alex Shoemaker (AbbVie) for helpful suggestions. T.J. is a Howard Hughes Medical Institute Investigator and a Daniel K. Ludwig Scholar. This work was supported by Dana Farber/Harvard Cancer Center (DF/HCC) Lung Cancer Specialized Program in Research Excellence NIH–National Cancer Institute (NCI) Grant 2P50 CA09057 (to J.A.E.); NIH Grants R01CA140594 (to J.A.E.), R01CA137008-01 (to J.A.E.), and 1U54HG006097-01 (to C.H.B.); Department of Defense Grants W81-XWH-13-1-0323 (to T.J.) and W81-XWH-13-1-0325 (to J.A.E.); U.S. Army Medical Research and Material Command Acquisition Activity is the awarding and administering acquisition office (T.J. and J.A.E.); Cancer Center Support Grant P30-CA14051 from the NCI (to T.J.); the David H. Koch Institute for Integrative Cancer Research at the Massachusetts Institute of Technology (Koch Institute)–DF/HCC Bridge Project (T.J. and J.A.E.); Grant 086357 from the Wellcome Trust (to C.H.B.); awards from the Burroughs Wellcome Fund and the Howard Hughes Medical Institute (to M.N.R.); a Lung Cancer Research Foundation grant (to A.C.F.); an American Cancer Society Postdoctoral Fellowship (to A.C.F.); and a grant from Uniting Against Lung Cancer (to A.F.F.).

1. Faber AC, Ebi H, Costa C, Engelman JA (2012) Apoptosis in targeted therapy responses: The role of BIM. *Adv Pharmacol* 65:519–542.
2. Faber AC, et al. (2011) BIM expression in treatment-naive cancers predicts responsiveness to kinase inhibitors. *Cancer Discov* 1(4):352–365.
3. Faber AC, et al. (2009) Differential induction of apoptosis in HER2 and EGFR addicted cancers following PI3K inhibition. *Proc Natl Acad Sci USA* 106(46):19503–19508.
4. Costa C, et al. (2014) The impact of EGFR T790M mutations and BIM mRNA expression on outcome in patients with EGFR-mutant NSCLC treated with erlotinib or chemotherapy in the randomized phase III EURTAC trial. *Clin Cancer Res* 20(7):2001–2010.
5. Tse C, et al. (2008) ABT-263: A potent and orally bioavailable Bcl-2 family inhibitor. *Cancer Res* 68(9):3421–3428.
6. Del Gaizo Moore V, et al. (2007) Chronic lymphocytic leukemia requires BCL2 to sequester prodeath BIM, explaining sensitivity to BCL2 antagonist ABT-737. *J Clin Invest* 117(1):112–121.
7. Faber AC, et al. (2014) mTOR inhibition specifically sensitizes colorectal cancers with KRAS or BRAF mutations to BCL-2/BCL-XL inhibition by suppressing MCL-1. *Cancer Discov* 4(1): 42–52.
8. Sale MJ, Cook SJ (2013) The BH3 mimetic ABT-263 synergizes with the MEK1/2 inhibitor selumetinib/AZD6244 to promote BIM-dependent tumour cell death and inhibit acquired resistance. *Biochem J* 450(2):285–294.
9. Chen S, Dai Y, Harada H, Dent P, Grant S (2007) Mcl-1 down-regulation potentiates ABT-737 lethality by cooperatively inducing Bak activation and Bax translocation. *Cancer Res* 67(2): 782–791.
10. Lin X, et al. (2007) 'Seed' analysis of off-target siRNAs reveals an essential role of Mcl-1 in resistance to the small-molecule Bcl-2/Bcl-XL inhibitor ABT-737. *Oncogene* 26(27):3972–3979.
11. Roberts AW, et al. (2012) Substantial susceptibility of chronic lymphocytic leukemia to BCL2 inhibition: Results of a phase I study of navitoclax in patients with relapsed or refractory disease. *J Clin Oncol* 30(5):488–496.
12. Al-Harbi S, et al. (2011) An antiapoptotic BCL-2 family expression index predicts the response of chronic lymphocytic leukemia to ABT-737. *Blood* 118(13):3579–3590.
13. Garnett MJ, et al. (2012) Systematic identification of genomic markers of drug sensitivity in cancer cells. *Nature* 483(7391):570–575.
14. Adams JM, et al. (2005) Subversion of the Bcl-2 life/death switch in cancer development and therapy. *Cold Spring Harb Symp Quant Biol* 70:469–477.
15. van Delft MF, et al. (2006) The BH3 mimetic ABT-737 targets selective Bcl-2 proteins and efficiently induces apoptosis via Bak/Bax if Mcl-1 is neutralized. *Cancer Cell* 10(5):389–399.
16. Mason KD, et al. (2008) In vivo efficacy of the Bcl-2 antagonist ABT-737 against aggressive Myc-driven lymphomas. *Proc Natl Acad Sci USA* 105(46):17961–17966.
17. Nguyen M, et al. (2007) Small molecule obatoclax (GX15-070) antagonizes MCL-1 and overcomes MCL-1-mediated resistance to apoptosis. *Proc Natl Acad Sci USA* 104(49):19512–19517.
18. Rodriguez E, Lilenbaum RC (2010) Small cell lung cancer: Past, present, and future. *Curr Oncol Rep* 12(5):327–334.
19. Shoemaker AR, et al. (2008) Activity of the Bcl-2 family inhibitor ABT-263 in a panel of small cell lung cancer xenograft models. *Clin Cancer Res* 14(11):3268–3277.
20. Sartorius UA, Krammer PH (2002) Upregulation of Bcl-2 is involved in the mediation of chemotherapy resistance in human small cell lung cancer cell lines. *Int J Cancer* 97(5):584–592.
21. Hann CL, et al. (2008) Therapeutic efficacy of ABT-737, a selective inhibitor of BCL-2, in small cell lung cancer. *Cancer Res* 68(7):2321–2328.
22. Gandhi L, et al. (2011) Phase I study of Navitoclax (ABT-263), a novel Bcl-2 family inhibitor, in patients with small-cell lung cancer and other solid tumors. *J Clin Oncol* 29(7):909–916.
23. Mason KD, et al. (2007) Programmed anuclear cell death delimits platelet life span. *Cell* 128(6):1173–1186.
24. Rudin CM, et al. (2012) Phase II study of single-agent navitoclax (ABT-263) and biomarker correlates in patients with relapsed small cell lung cancer. *Clin Cancer Res* 18(11):3163–3169.
25. McCoy F, et al. (2010) Obatoclax induces Atg7-dependent autophagy independent of beclin-1 and BAX/BAK. *Cell Death Dis* 1:e108.
26. Hwang JJ, et al. (2010) Phase I dose finding studies of obatoclax (GX15-070), a small molecule pan-BCL-2 family antagonist, in patients with advanced solid tumors or lymphoma. *Clin Cancer Res* 16(15):4038–4045.
27. Paik PK, et al. (2011) A phase II study of obatoclax mesylate, a Bcl-2 antagonist, plus topotecan in relapsed small cell lung cancer. *Lung Cancer* 74(3):481–485.
28. Wendel HG, et al. (2007) Dissecting eIF4E action in tumorigenesis. *Genes Dev* 21(24): 3232–3237.
29. Schatz JH, et al. (2011) Targeting cap-dependent translation blocks converging survival signals by AKT and PIM kinases in lymphoma. *J Exp Med* 208(9):1799–1807.
30. Mills JR, et al. (2008) mTORC1 promotes survival through translational control of Mcl-1. *Proc Natl Acad Sci USA* 105(31):10853–10858.
31. Hsieh AC, et al. (2010) Genetic dissection of the oncogenic mTOR pathway reveals druggable addiction to translational control via 4EBP-eIF4E. *Cancer Cell* 17(3): 249–261.
32. Chresta CM, et al. (2010) AZD8055 is a potent, selective, and orally bioavailable ATP-competitive mammalian target of rapamycin kinase inhibitor with in vitro and in vivo antitumor activity. *Cancer Res* 70(1):288–298.
33. Choo AY, Yoon SO, Kim SG, Roux PP, Blenis J (2008) Rapamycin differentially inhibits S6Ks and 4E-BP1 to mediate cell-type-specific repression of mRNA translation. *Proc Natl Acad Sci USA* 105(45):17414–17419.
34. Cope CL, et al. (2014) Adaptation to mTOR kinase inhibitors by amplification of eIF4E to maintain cap-dependent translation. *J Cell Sci* 127(Pt 4):788–800.
35. Gardner EE, et al. (2014) Rapamycin rescues ABT-737 efficacy in small cell lung cancer. *Cancer Res* 74(10):2846–2856.
36. Meuwissen R, et al. (2003) Induction of small cell lung cancer by somatic inactivation of both Trp53 and Rb1 in a conditional mouse model. *Cancer Cell* 4(3):181–189.
37. Sutherland KD, et al. (2011) Cell of origin of small cell lung cancer: Inactivation of Trp53 and Rb1 in distinct cell types of adult mouse lung. *Cancer Cell* 19(6):754–764.
38. Dooley AL, et al. (2011) Nuclear factor I/B is an oncogene in small cell lung cancer. *Genes Dev* 25(14):1470–1475.
39. McFadden DG, et al. (2014) Genetic and clonal dissection of murine small cell lung carcinoma progression by genome sequencing. *Cell* 156(6):1298–1311.
40. Peifer M, et al. (2012) Integrative genome analyses identify key somatic driver mutations of small-cell lung cancer. *Nat Genet* 44(10):1104–1110.
41. Rudin CM, et al. (2012) Comprehensive genomic analysis identifies SOX2 as a frequently amplified gene in small-cell lung cancer. *Nat Genet* 44(10):1111–1116.
42. Hanna N, et al. (2006) Randomized phase III trial comparing irinotecan/cisplatin with etoposide/cisplatin in patients with previously untreated extensive-stage disease small-cell lung cancer. *J Clin Oncol* 24(13):2038–2043.
43. Singh M, et al. (2012) Anti-VEGF antibody therapy does not promote metastasis in genetically engineered mouse tumour models. *J Pathol* 227(4):417–430.
44. Rossi A, et al. (2012) Carboplatin- or cisplatin-based chemotherapy in first-line treatment of small-cell lung cancer: The COCIS meta-analysis of individual patient data. *J Clin Oncol* 30(14):1692–1698.
45. Barretina J, et al. (2012) The Cancer Cell Line Encyclopedia enables predictive modelling of anticancer drug sensitivity. *Nature* 483(7391):603–607.

Supporting Appendix for:

Assessment of ABT-263 activity across a cancer cell line collection leads to a potent combination therapy for small cell lung cancer.

Anthony C. Faber[1,2*#], Anna F. Farago[1,2,3*], Carlotta Costa[1,2*], Anahita Dastur[1,2], Maria Gomez-Caraballo[1,2], Rebecca Robbins[3], Bethany L. Wagner[3], William M. Rideout, 3rd[3], Charles T. Jakubik[1,2], Jungoh Ham[1,2], Elena J. Edelman[1,2], Hiromichi Ebi[1,2+], Alan T. Yeo[1,2], Aaron N. Hata[1,2], Youngchul Song[1,2], Neha U. Patel[4], Ryan J. March[1,2], Ah Ting Tam[1,2], Randy J. Milano[1,2], Jessica L. Boisvert[1,2], Mark A. Hicks[4], Sarah Elmiligy[3], Scott E. Malstrom[3], Miguel N. Rivera[1,5], Hisashi Harada[4], Brad E. Windle[4], Sridhar Ramaswamy[1,2], Cyril H. Benes[1,2], Tyler Jacks[3] and Jeffrey A. Engelman[1,2]

Supporting Appendix contents:

Supporting Figure Legends.

Supporting Figure 1. *BIM/MCL-1* ratios predict sensitivity to ABT-263 in an independent gene expression data set. (A) Scatter plot of ABT-263 IC50 (μM) values plotted on a natural log scale versus relative *BIM* expression levels measured from Wooster et al. (https://www.oncomine.com/) (n=133). A linear regression analysis was used to assign a coefficient of determination (R^2) of 0.059 and a P value of 0.0048. (B) Scatter plot of ABT-263 IC50 (μM) values on the natural log scale versus relative *MCL-1* RNA expression levels measured from the CCLE[45]. A linear regression analysis was used to assign a coefficient of determination (R^2) of 0.097 and a P value of 2.22e-08. (C) Scatter plot of ABT-263 IC50 (μM) values plotted on a natural log scale versus relative *MCL-1* RNA expression levels using the gene expression set from Wooster et al. A linear regression analysis was used to assign a coefficient of determination (R^2) of 0.115 and a P value of 6.91e-05. (D) Scatter plot of ABT-263 IC50 (μM) values on the natural log scale versus the ratio of *BIM*/*MCL-1* expression levels. A linear regression analysis was used to assign a coefficient of determination (R^2) of 0.164 and a P value of 1.28e-06. Expression levels were from Wooster et al. (E) Scatter plots comparing IC50 (μM) values plotted on a natural log scale between cell lines with high *BIM* expression (top 20%) and low *MCL-1* expression (cut-off at the median), cell lines with high *BIM* expression (top 20%) and high *MCL-1* expression (cut-off at the median), and cell lines with low *BIM* expression and low *MCL-1* expression. Expression levels of *BIM* and *MCL-1* represent the data by Wooster et al. The red bars indicate the geometric means of the IC50s for each group of cell lines. An unpaired t-test with Welch's correction was used to assign a

P value for differential IC50s between the *BIM* high/*MCL-1* low group and the two other groups, P =0.039 and P =0.0141, respectively.

Supporting Figure 2. BIM/MCL-1 is a superior predictor of sensitivity to ABT-263 across solid tumor cancer cell lines. Scatter plot of ABT-263 IC50 (μM) values plotted on a natural log scale versus (A) relative *BIM* expression levels (B) relative *BIM*/*MCL-1* expression levels (C) relative BCL-XL levels (D) relative *BCL-XL*/*MCL-1* levels (E) *BCL-2* levels and (F) relative BCL-2/MCL-1 levels of all solid tumor cell lines. Expression levels were taken from the CCLE[45]. A linear regression analysis was used to assign a coefficient of determination (R^2) of 0.024 and P value of 0.0103 for (A), an R^2 of 0.069 and a P value of <0.0001 for (B), an R^2 of 0.001 and a P value of 0.4018 (P=NS) for (C), an R^2 of 0.009 and a P value of 0.2156 (P=NS) for (D), an R^2 of 0.010 and a P value of 0.0961 (P=NS) for (E), and a R^2 of 0.040 and a P value of 0.0009 for (F).

Supporting Figure 3. SCLC cells express high levels of BIM compared to other solid tumor cancers. Box plot showing increased expression of *BIM* in SCLC cell lines compared to other solid tumors using the dataset from Wooster et al. (https://www.oncomine.com/) . A Wilcoxon rank sum test was used to assign a P value of 0.001 between the two groups.

Supporting Figure 4. ABT-263 has anti-cancerous effects in different cancers, and has enhanced activity in SCLC. Key for different cancer types shown in Figure 1E.

Supporting Figure 5. A second BIM siRNA reduces ABT-263-induced apoptosis, BIM Ab binds to and immunoprecipitates BIM, and elevated MCL-1 levels in SCLC. **(A)** SCLC SW1271 and H1048 cells were treated with either 50 nM scrambled (sc) or *BIM* siRNA (Dharmacon), and, the next day, cells were treated with or without ABT-263. Then, (A) cells were prepared and stained with propidium iodide and Annexin-V. Apoptosis was measured by FACS analysis of percent of cells positive for Annexin-V 72 h after treatment, (the amount of apoptotic cells caused by ABT-263 treatment minus no drug treatment), or (B) lysed and separated by SDS-PAGE, subjected to Western blot, and probed with the indicated antibodies. (C) Western blot analysis of H1048 cells expressing GFP alone (GFP) or GFP-IRES-MCL-1 ("low") and ("high"). The H82 cell line is included for comparision. (D) Equal amounts of H1048 protein extracts ("E") prior to BIM immunoprecipitation (Fig. 2E) and in the resultant supernatant ("S") were probed with the indicated antibodies. (E) Box plot showing increased expression of MCL-1 in SCLC cell lines compared to other solid tumors. A Wilcoxon rank sum test was used to assign a P value for differential expression between the two groups, P value of 1.24e-05. Expression values were taken from the CCLE[45].

Supporting Figure 6. MCL-1 affects ABT-263 sensitivity, and AZD8055 disrupts ABT-263-mediated accumulation of BIM:MCL-1 complexes. (A) SCLC H1048 cells were treated with either 100 nM scrambled (sc) or *MCL-1* siRNA (Cell Signaling Technologies) for 24 h. Cells were either (left) re-seeded and treated the following day with no drug (control) or ABT-263 and prepared for FACS analysis of percent of cells with Annexin-V positivity 24 hours after treatment or (right) cell lysates were prepared

from the transfected cells and separated by SDS-PAGE, subjected to Western blot, and probed with the indicated antibodies. Error bars are S.D (n=3). (B) H446 and H196 SCLC cells were treated with no drug (-), 1 μM ABT-263, 500 nM AZD8055, or 500 nM AZD8055/1 μM ABT-263 for 6 h, and lysates were immunoprecipitated with BIM. Precipitates were analyzed by Western blot analyses with the indicated antibodies. (C) H446 and H196 cells transduced with lentiviral particles expressing GFP alone (GFP) or GFP-IRES-MCL-1 (MCL-1) were treated with either no drug (control) or 500 nM AZD8055/1 μM ABT-263. Following 72 h of treatment, cells were prepared and stained with propidium iodide and Annexin-V, and apoptosis was measured by FACS analysis of percent of cells with Annexin-V positivity. Bars represent mean percent of apoptotic cells following combination treatment over control. Error bars are S.D. (n=3). (D) H446 and H196 cells were transduced with lentiviral particles expressing GFP alone (GFP) or GFP-IRES-MCL-1 (MCL-1) (the same cells as in (C)), and cell lysates were prepared from the transfected cells and separated by SDS-PAGE, subjected to Western blot, and probed with the indicated antibodies.

Supporting Figure 7. AZD8055/ABT-263 induces growth arrest in SCLC. SCLC cell line (A) H82, (B) H1048 and (C) H196 were treated with no drug (Media), 500 nM AZD8055, 1 μM ABT-263, or 500 nM AZD8055/1 μM ABT-263 for 24 hours and the percent of cells in each phase of the cell cycle was determined by PI staining followed by FACS analysis. Bars are percent of cells in S phase. Error bars are S.D. (n=3). *= $P<0.05$ for control versus combination-treated cells, Student's *t* test.

Supporting Figure 8. Rapamycin is not equivalent to AZD8055 in combination with ABT-263 to induce apoptosis in SCLC, and lack of BAX involvement in AZD8055-induced apoptosis. (A and B) SCLC cell lines H196, H1048, H82 and H446 were treated with no drug (-), 500 nM AZD8055, 1 μM ABT-263, 500 nM AZD8055/1 μM ABT-263, 200 nM rapamycin, or 200 nM rapamycin/1 μM ABT-263. (A) After 16 h, lysates were prepared and subjected to Western blot analyses and probed with the indicated antibodies. Note: "loading" either GAPDH or β -ACTIN antibodies. (B) After 48 h, H196 and H1048 cells were prepared and stained with propidium iodide and Annexin-V, and apoptosis was measured by FACS analysis of percent of cells with Annexin-V positivity. Values shown are the percent of apoptosis induced by each agent above control. Error bars are S.D. (n=3). *= $P<0.001$ for rapamycin/ABT-263 versus AZD8055/ABT-263-treated cells, Student's *t* test. (C) H1048 and H196 cells were treated with no drug (-), 500 nM AZD8055, 1 μM ABT-263, 500 nM AZD8055/1 μM ABT-263, 200 nM rapamycin, or 200 nM rapamycin/1 μM ABT-263 for 16 h, and lysates were prepared and subjected to Western blot analyses and probed with the indicated antibodies. (D) H1048 cells were treated with no drug (-), 500 nM AZD8055, 1 μM ABT-263, or 500 nM AZD8055/1 μM ABT-263 for 16 hours and cells were prepared and stained with propidium iodide and Annexin-V, and apoptosis was measured by FACS analysis of percent of cells with Annexin-V positivity. Values shown are the percent of apoptosis induced by each agent above control. Error bars are S.D. (n=3). Note: Induction of significant apoptosis of the combination at 16 hours despite no marked changes in BAX expression.

Supporting Figure 9. MCL-1 loss is consistent with protein translation block. (A) H1048 cells were not treated (-), treated with 10μg/mL CHX for 1,2 4, or 6 hours in the presence or absence of 500 nM AZD8055 (CHX+AZD8055), or AZD8055 alone for 6 hours and lysates were prepared and subjected to Western blot analyses and probed with the indicated antibodies. (B) MCL-1 and β-ACTIN band intensities were quantified on a Syngene and the ratio is shown.

Supporting Figure 10. AZD8055/ABT-263 induces apoptosis in SCLC *in vivo* without overt toxicity. (A) Tumors from H1048 xenografts were stained for CC3 as noted in the Fig. 3G legend. The number of CC3-positive cells was determined by a blinded investigator using three non-overlapping 40X images (examples are shown in Figure 3G) from mice in each treatment cohort. The percent of CC3-positive cells are represented by each bar. Error bars are + S.E.M. (n=3). * = P <0.05, ABT-263 versus combination treatment group, Student's *t*-test. (B) Mouse weights from H1048 xenografts presented in Figure 3E of the mice that underwent combination treatment (n=4). There were no significant differences in the weights of mice during the course of treatment (Student's *t*-test, n=4, NS= not significant, day 0 weight versus the indicated day). Error bars are S.D.

Supporting Figure 11. Cell lines established from a SCLC GEMM downregulate MCL-1 following AZD8055 treatment and are sensitized to ABT-263 by the addition of AZD8055. (A) The three indicated murine SCLC cell lines (984-LN, H4600-T1, and AF1077) were treated with no drug (no Rx), 500 nM AZD8055, 1 μM ABT-263, or

combination 500 nM AZD8055/1 μM ABT-263 and after 16 h of treatment, lysates were probed with the indicated antibodies. (B) Murine SCLC cell lines were treated with no drug (media), 100 nM ABT-263 (ABT-263 only), or 100 nM ABT-263 in combination with the indicated dose of AZD8055 (ranging from 1.66 nM to 5000 nM AZD8055) for seven days. The number of viable cells was determined by CellTiter-Glo® and presented as fold-change of cells compared to day 0 (i.e., negative values represent loss of cells from day 0). Error bars are S.D. of cells treated in triplicate.

Supporting Figure 12. SCLC PDX model growth prior to treatment start. NSG mice engrafted with tumor pieces from a SCLC patient were monitored for tumor growth. Shown in the graph are the 7 days of tumor measurements prior to treatment start. Percent of tumor growth is shown next to the line representing the respected tumor. Please note: Blue is ABT-263 monotherapy, red is combination ABT-263 and AZD8055. *indicates the tumor growth change is for the 10 days prior to treatment start for that tumor (the first three days are not graphed), as this tumor began growing earlier then the other tumors monitored.

Supporting Figure 13. SCLC cells are sensitized to AZD8055 by addition of ABT-263. H1048 SCLC cells were treated with no drug (Media), 50 nM AZD8055, or 50 nM AZD8055 in combination with the indicated dose range of ABT-263 (ranging from 3.3 nM to 10 uM ABT-263) for seven days. The number of viable cells were determined by CellTiter-Glo®, and presented as fold-change of cells compared to day 0 (i.e., negative values represent loss of cells from day 0). Error bars are S.D. of cells treated in triplicate.

Materials and Methods

Cell lines

NCI-H82, NCI-H446, NCI-H196, DMS79, NCI-H209, NCI-H211 and NCI-H146 cells were cultured in RPMI (Sigma-Aldrich). SW1271 and NCI-H1048 cells were cultured in Dulbecco's Modified Eagle Medium (DMEM) (Invitrogen). NCI-H1092 cells were cultured in DMEM supplemented with 4ug/mL Hydrocortisone and Insulin-Transferrin-Selennium Mix (Invitrogen) at 1:100. All the FBS concentrations were 10%. All the human cell lines were from the Center for Molecular Therapeutics[13] at Massachusetts General Hospital Cancer Center. Murine SCLC cell lines were generated as previously described[39].

Antibodies and reagents

The antibodies used in this study included phospho-4E-BP1 (37/46), phospho-S6 (240/244), total 4E-BP1, total S6 and cleaved caspase 3, which were from Cell Signaling Technology (Beverly, MA). Antibodies from Cell Signaling used to probe nitrocellulose membranes following Western blotting were all used at 1:1000 dillutions. GAPDH 1:3000 dillution (Mab 374, Millipore) or β-ACTIN (Cell Signaling, 1:1000) were used as internal loading controls. MCL-1 (S19) and BAX (N-20) (Santa Cruz Biotechnology) were used at a 1:200 dillution and 1:500 dillution, respectively. The diluent for all Abs was TBS-T with 5% BSA and .01% Sodium Azide, both of which from Sigma-Aldrich (St. Louis, MO). BIM siRNA and scramble siRNA were from Qiagen for Figure 2A and 2B, and GE Dharmacon (Lafayette, CO) for Sup. Figure 5A and 5B. The MCL-1 siRNA and scramble siRNA was from GE Dharmacon for Figure 2I and the MCL-1 siRNA and

scramble siRNA was from Cell Signaling and Qiagen, respectively, for Sup. Figure 6A. For FACS experiments, Annexin-Cy5 was from Biosource International (Camarillo, CA) and FITC-Annexin was from BD Biosciences (San Jose, CA). Propidium iodide (PI) was from Sigma-Aldrich and BD Biosciences. ABT-263 and AZD8055 were purchased from Active Biochemicals (Hong Kong, China) and Abmole Bioscience (Houston, TX). Captisol ® was purchased from Ligand Technology and was used to dissolve AZD8055 for *in vivo* experiments.

Western blotting

Prior to Western blotting, cell lines and tumors from the traditional human xenografts and patient-derived xenograft were prepared and lysed as previously described[3]. Proteins were resolved using the NuPAGE® Novex® *Midi Gel system* on 4-12% BIS-TRIS gels (Invitrogen, Carlsbad, CA). Chemiluminescence (SuperSignal West Femto Chemiluminescent Substrate, Thermo Scientific, Rockford, IL) was detected with the Syngene G:Box camera (Syngene USA, Frederick, MA), and chemiluminescent signal intensity was quantified with Syngene Genetools software (Syngene USA) where indicated, normalized to GAPDH or β-ACTIN loading control.

Immunoprecipitation (IP)

Cells were lysed in the same buffer as used for Western blotting experiments. 20uL of protein A sepharose beads (GE Healthcare, Bio-Sciences, Pittsburgh, PA) were added to an equal amount of cellular lysates, followed by 5μg of BIM antibody (cat# 2819, Cell Signaling, Beverly, MA) or, when indicated, IgG isotype control. Following incubation

with motion at 4 degrees Celsius, supernatant was collected and the IP complexes were washed three times in cold PBS, boiled, and ran on a 4-12% BIS-TRIS gel (Invitrogen, Carlsbad, CA). Remaining cellular lysates not subjected to immunoprecipitation (for Fig. 2E) were analyzed next to the corresponding supernatant from the immunoprecipitation.

RNA extraction and quantitative (q)RT-PCR

RNA was isolated from cultured cells grown at sub-confluency using the Qiagen RNeasy Mini kit and subsequently DNAse-treated as described previously[3]. Isolated RNA was reverse-transcribed and amplified using first-strand cDNA synthesis (Invitrogen, Carlsbad, CA). The numbers of *BIM* and *MCL-1* molecules were monitored in real time on a Roche Lightcycler 480 (Roche Diagnostics) by measuring the fluorescence increases of Sybr Green (Roche Diagnostics). The number of *β-Actin* molecules was also measured in parallel. The primers used were: *BIM* Forward (5'-AGTCCTTCCAGTGGGTATTTCTCTT-3') and *BIM* Reverse (5'-ACTGAGATAGTGGTTGAAGGCCTGG-3'); MCL-1 Forward (5'-GGGCAGGATTGTGACTCTCATT-3'); MCL-1 Reverse (5'-GATGCAGCTTTCTTGGTTTATGG); *β-Actin* Forward (5'-CTGTGCTATCCCTGTACGCCTC-3') and *β-Actin* Reverse (5'-CATGATGGAGTTGAAGGTAGTTTCTG-3'). To determine relative abundance of *BIM* and *MCL-1* RNA molecules, the $\Delta\Delta CT$ method was utilized.

Cell Viability

The drug screen conducted by the Center for Molecular Therapeutics at the Massachusetts General Hospital Cancer Center has been described[13]. For the other cell viability determinations, cells were seeded sparsely in two flat-bottom black 96-well plates per experiment. The cells in one plate were treated the next day with drug, and in the second plate 50μL of CellTiter-Glo assay (Promega, Madison, WI) was added per well and immediately placed at -80 Celsius. Following seven days of continuous drug treatment at 37 degrees Celsius, and 5% atmospheric CO_2, 50μL of CellTiter-Glo was added to each well of cells from the first plate and immediately placed at -80 Celsius. Cells were subsequently thawed on a rocker and upon thawing, were read on a Centro LB 960 microplate luminometer (Berthold Technologies, Oak Ridge, TN) according to the Promega protocol.

MCL-1 overexpression

MCL-1 in a pcDNA3 vector was kindly provided by Dr. Gordon Shore (Department of Biochemistry, McGill University). MCL-1 was subcloned into pENTR/TOPO vector, and recombined into pLENTI-GFP by Clonase reaction (Invitrogen), and subsequently FACS sorted for GFP expression.

Flourescence Activated Cell Sorting (FACS) for death assays and cell cycle analysis

Cells were plated in triplicate in 6-well plates or 6-cm dishes to reach ~30-40% confluency the next day. On the next day, cells were treated with the indicated drugs or no drug control. Apoptosis and cell cycle experiments were performed essentially as previously described[3] and analyzed on a BD LSR III (Becton Dickenson, Franklin Lanes,

NJ). The cell cycle experiments were gated to include only viable cells in order for the cell cycle distribution to be determined from this population. For apoptosis assays, the number of cells in quadrants II and IV (Annexin positive) were counted as apoptotic, with the exception of apoptosis experiments in Figure 2F-2H, where cells with sub-G0/G1 DNA[3] were quantified and counted as apoptotic following staining with PI. For the data from Supplemental Figures 5A, 6A and 8D, the Annexin stain was conjugated to FITC and the analysis was done on a Guava easyCyte flow cytometer (EMD Millipore (Temecula, CA)). In the engineered H1048 cells, apoptosis determined by ABT-263 treatment (Fig. 2D) and combination ABT-263/AZD8055 treatment (Fig. 3D) were performed within the same experiment.

Traditional human cell-line xenograft experiments

6-10 week-old mice with a Nu/Nu background were injected subcutaneously with exponentially growing NCI-H1048 or NCI-H82 cells into the right rear flanks. Approximately 5,000,000 cells re-suspended in .2mL of PBS or .2mL PBS/matrigel (1:1) were injected. Tumors were monitored until they reached approximately 100-200mm^3. At this time, mice were separated into four groups (or three where indicated, Figure 6D): No treatment (control), AZD8055 only, ABT-263 only or combination treatment. Treatment doses are indicated in the figure legends for each experiment. AZD8055 was given approximately 1.5 h prior to ABT-263 for combination treatments. AZD8055 was dissolved in Captisol ®. ABT-263 was dissolved in a mixture of 60% Phosal 50 PG, 30% PEG 400 and 10% EtOH. Drugs were stored at 4 degrees Celsius and routinely no longer than one week after dissolving. Tumors were measured using electronic calipers in two-

dimensions (length and width), and with the formula: $v = l \times (w)^2 \times 0.52$ where v = tumor volume, l = length, and w =width.

Patient-derived xenografts

Female NOD *scid* gamma (NSG) mice were inoculated with tumor pieces derived from a tumor of a SCLC patient (Jackson laboratories, Bar Harbor, Maine). Upon arrival to Massachusetts General Hospital, tumor growth was carefully monitored and we identified eight mice with tumors growing to treatable levels (~150-300 mm^3)**.** These mice were then randomized into two groups; ABT-263 only or AZD8055/ABT-263 combination treatment. Treatment doses are indicated in the figure legend. AZD8055 was given approximately 1.5 h prior to ABT-263 for combination treatments. AZD8055 was dissolved in Captisol ®. ABT-263 was dissolved in a mixture of 60% Phosal 50 PG, 30% PEG 400 and 10% EtOH. Drugs were stored at 4 degrees Celsius and routinely no longer than one week after dissolving. Tumors were measured using electronic calipers in two-dimensions (length and width), and with the formula: $v = l \times (w)^2 \times 0.52$ where v = tumor volume, l = length, and w =width. For the Western blot analysis (Fig. 5B), tumors from two mice which grew following the beginning of the efficacy studies were collected and used as the no treatment controls.

Genetically engineered mouse model

$Tp53^{fl/fl}$; $Rb1^{fl/fl}$ mice have previously been described[38]. Tumors were initiated by intratracheal administration of Adenovirus expressing Cre recombinase under the control of either a CMV promoter or a CGRP (neuroendocrine cell specific) promoter[37] (Fig. 4A).

Viruses were titered to levels such that most animals developed exactly one radiographically measurable primary tumor in the lungs (Sup. Table 1). Tumor-bearing animals were identified by computed tomography (CT) scanning using the GE eXplore CT 120 Micro-CT (General Electric). Mice were then randomized to receive no treatment, ABT-263 (80 mg/kg by oral gavage daily 6 days per week), AZD8055 (16 mg/kg by oral gavage daily 6 days per week), or both AZD8055 and ABT-263 (given sequentially). Drugs were prepared as described above. Magnetic resonance imaging was performed and Varian 7T/310/ASR MRI system (Varian/Agilent Technologies). Images were analyzed and volumes computed using OsiriX (Pixmeo Sarl) v.5.7.1 32-bit. Following the prescribed course of treatment and follow-up MRI scan, animals were euthanized and tissues were collected for histologic review. For murine allograft experiments, SCLC GEMM primary lung tumors were dissected and a 2 mm x 2mm portion was subcutaneously implanted into an NSG recipient (Charles River). Once the implanted tumor reached 1 cm in diameter, 2 mm x 2 mm portions were dissected out and then passaged into nu/nu recipients (Charles River). The Massachusetts Institute of Technology (MIT) Institutional Animal Care and Use Committee approved all animal studies and procedures.

Histopathology and immunohistochemistry

FOR IHC performed on human cell lines, following mouse sacrifice and tumor collection, tissue was fixed in paraformaldehyde overnight, and stored in 70% EtOH until embedment. The tissue was embedded in paraffin, and sectioned at the Department of Pathology, Massachusetts General Hospital. Apoptosis was determined by cleaved

caspase 3 (CC3) positivity. The mTORC1 targets P4E-BP1 (37/36) and PS6 (240/4) antibodies were used to confirm AZD8055 activity *in vivo* on snap-frozen tumor removed directly following mouse sacrifice. Tissues were collected approximately 3 hours after the indicated treatments. IHC for CC3 in the GEMM SCLC allografted tumors was performed as previously described[39] using Cell Signaling Technology antibody #9661 at a dilution of 1:200.

Statistical Considerations

For the analyses of BIM and MCL-1 expression among cell lines and correlations to ABT-263 IC50s, we wanted to capture a significant number of just the most extreme expressors of BIM and therefore chose a cutoff of the top 10% (n=31) for the CCLE set, and 20% (n=27) for the Wooster set. We then wanted to further categorize these cell lines by those with high or low MCL-1 expression. In order to have an adequate number of cell lines in each group for comparisons we chose cutoffs of the top and bottom 25% of MCL-1 expression for the CCLE set (n=331) and 50% for the Wooster set (n=133). IC50s for cell lines were calculated as previously described in the drug screens[13]. Statistical tests in this study were linear regression analysis, student's t test, unpaired t-test with Welch's correction, and Wilcoxon rank sum tests. Differences were considered statistically different if $P<0.05$.

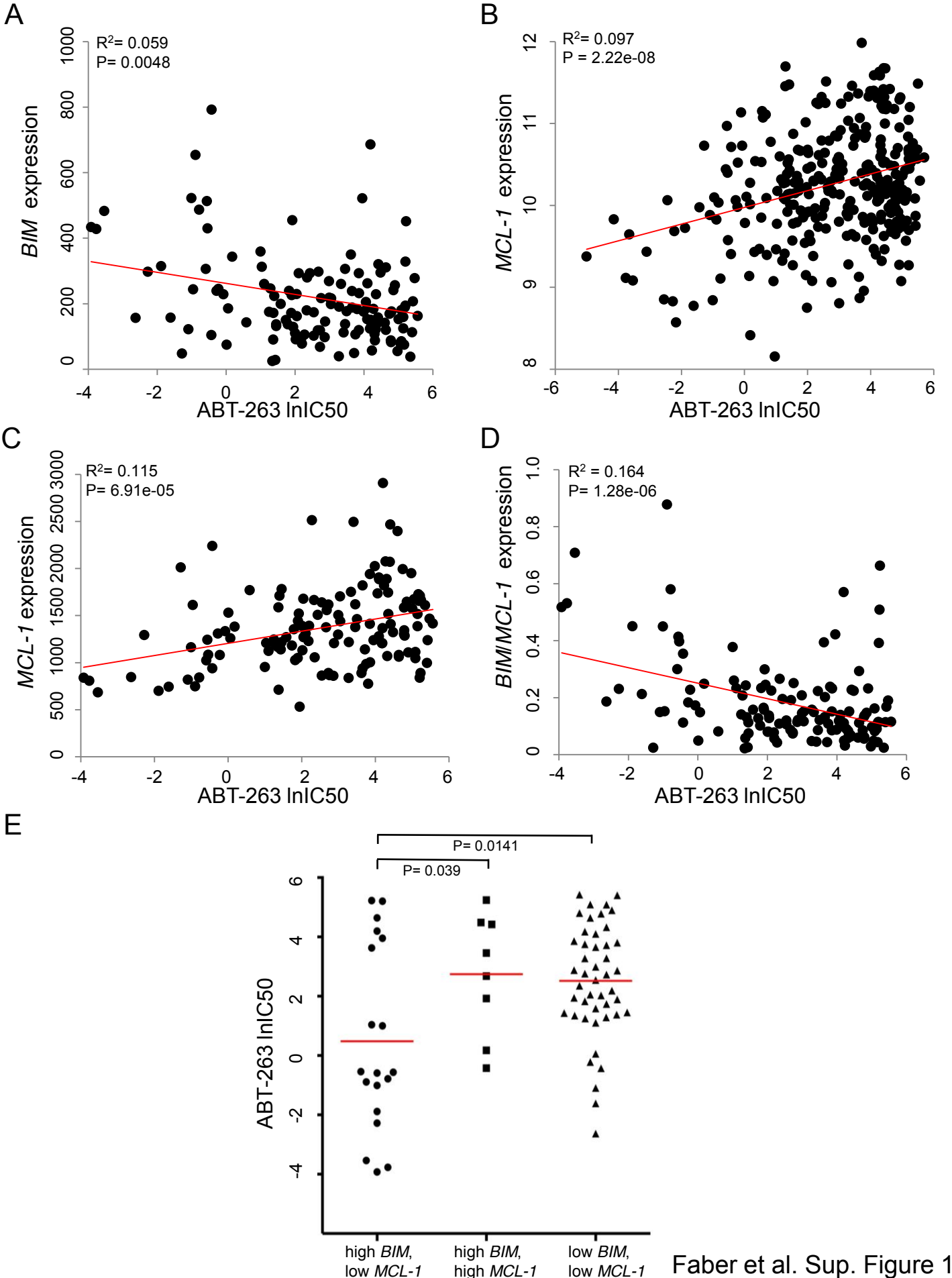

Faber et al. Sup. Figure 1

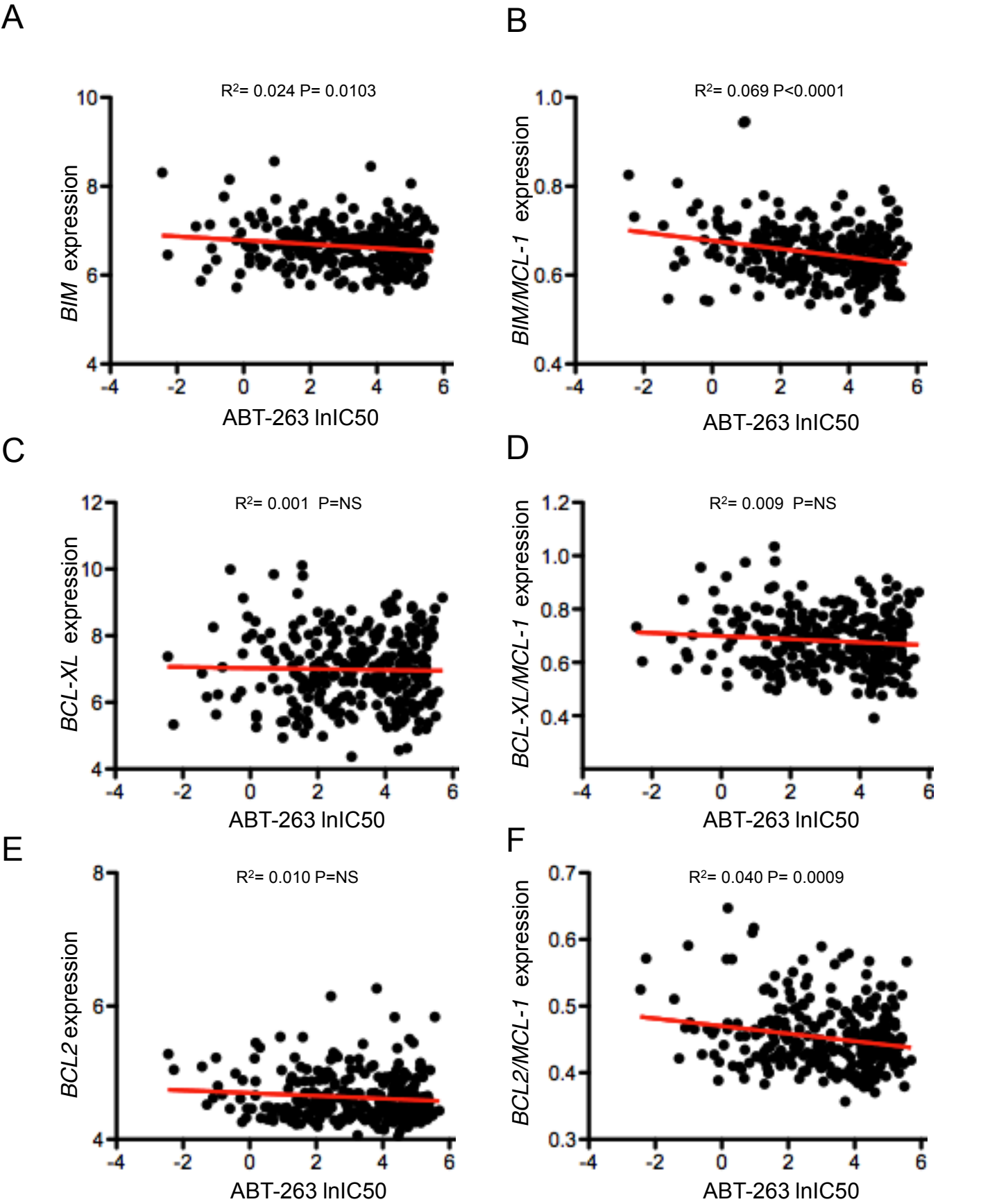

Faber et al. Sup. Figure 2

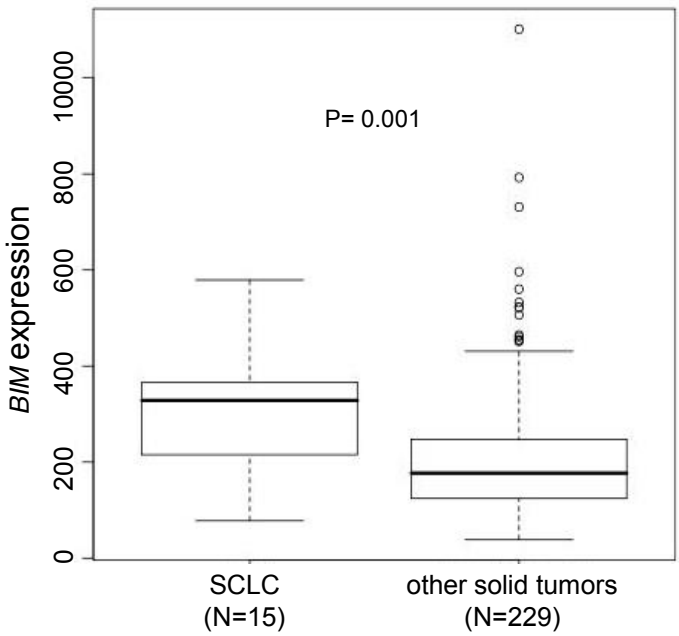

Faber et al. Sup. Figure 3

#	Cancer type
1	biliary tract
2	bladder
3	breast
4	cervix
5	kidney (clear cell)
6	endometrium
7	glioma
8	large intestine
9	liver
10	malignant melanoma
11	medulloblastoma
12	mesothelioma
13	neuroblastoma
14	non-small cell lung cancer
15	oesophagus
16	osteosarcoma
17	ovary
18	pancreas
19	prostate
20	kidney (renal cell)
21	small cell lung cancer
22	soft tissue (other)
23	stomach
24	thyroid
25	upper aerodigestive tract

Faber et al. Sup. Figure 4

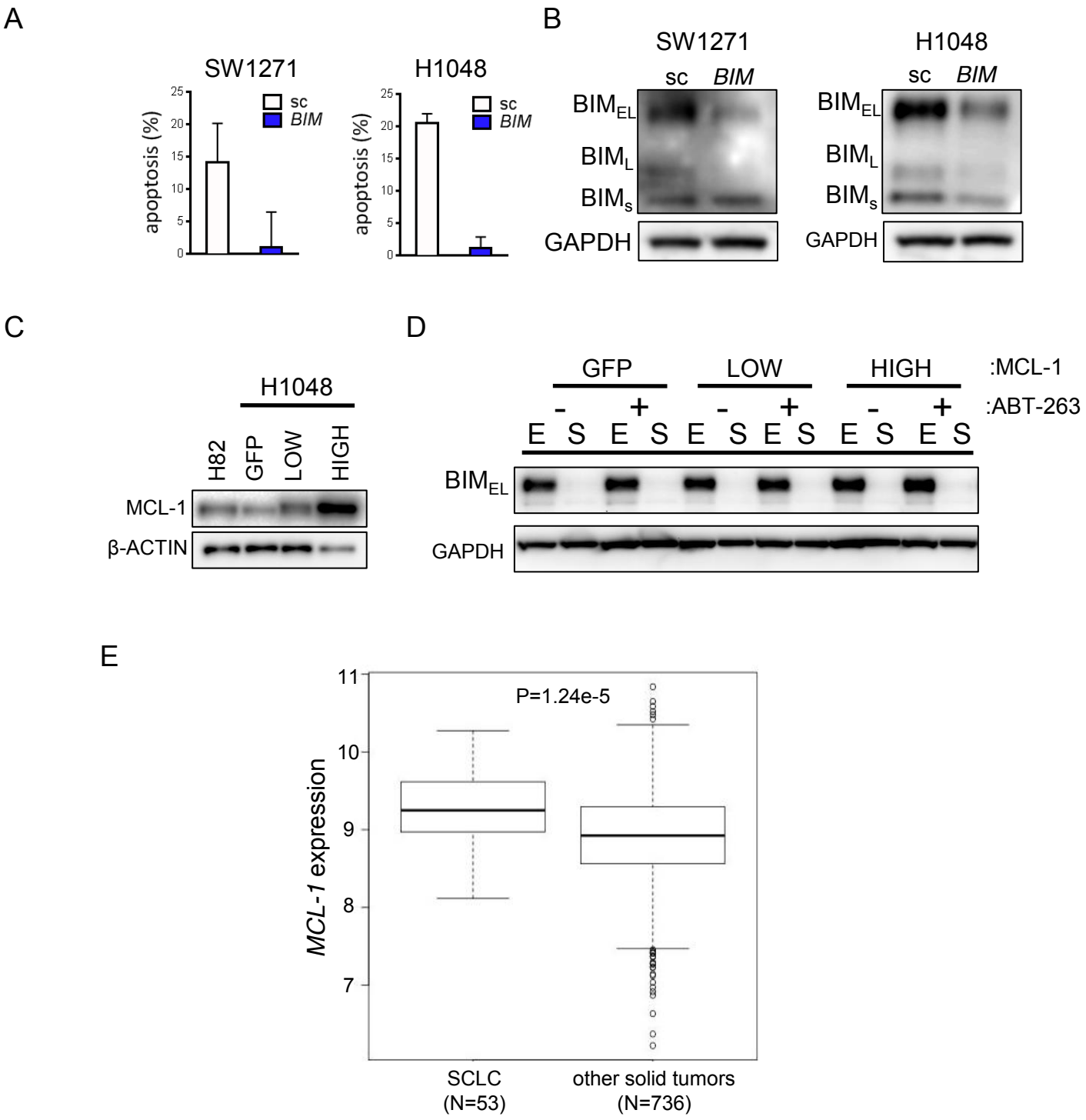

Faber et al. Sup. Figure 5

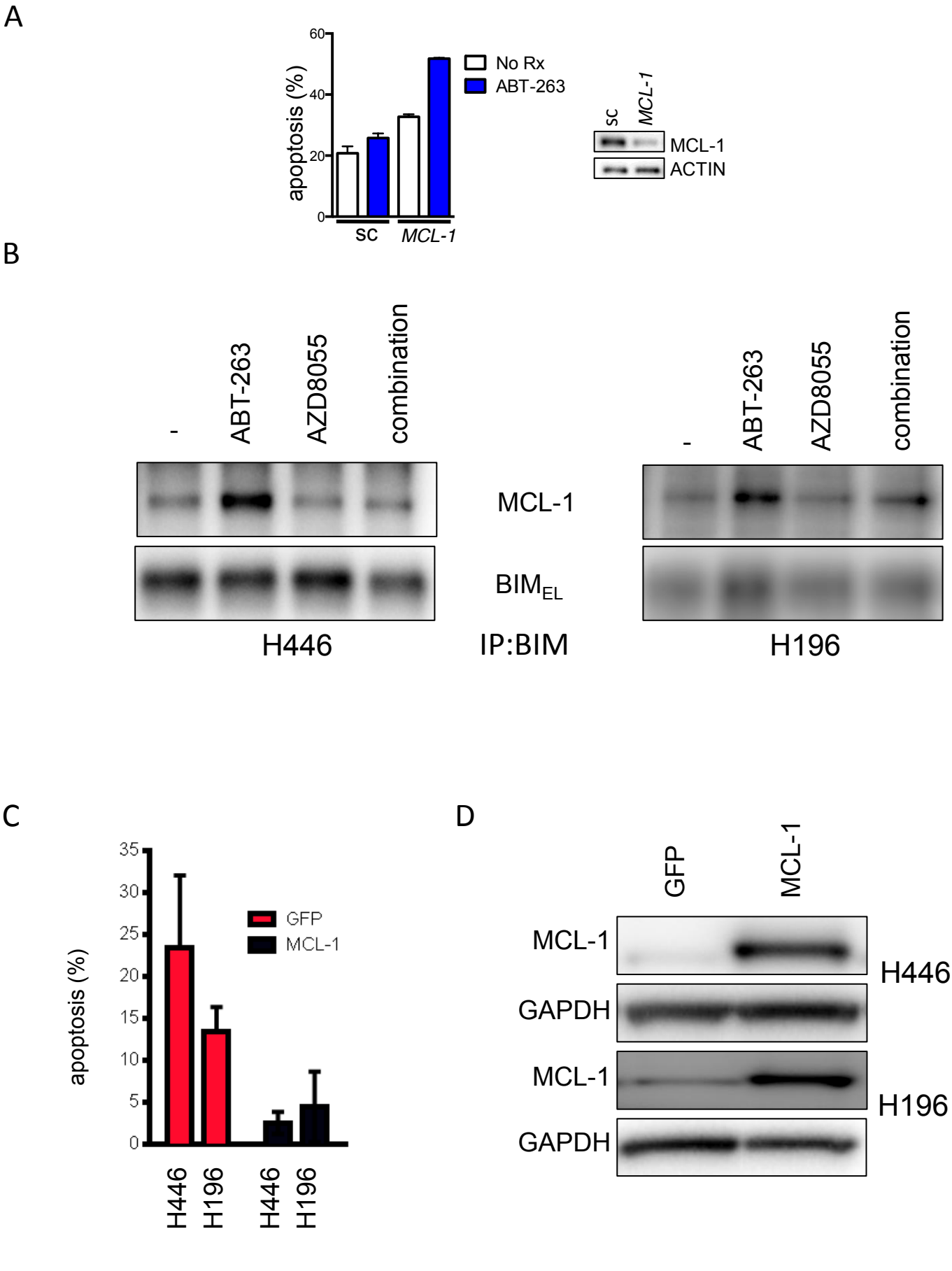

Faber et al. Sup. Figure 6

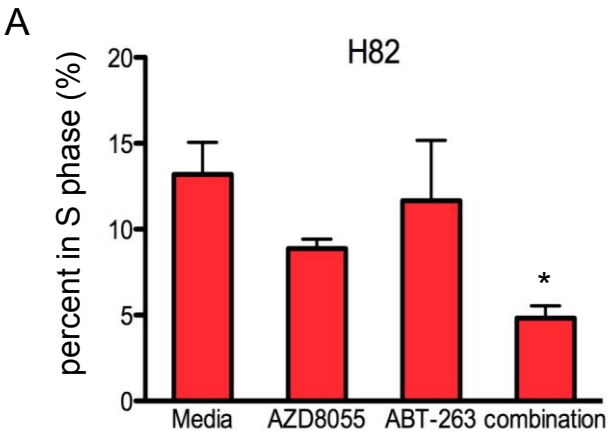

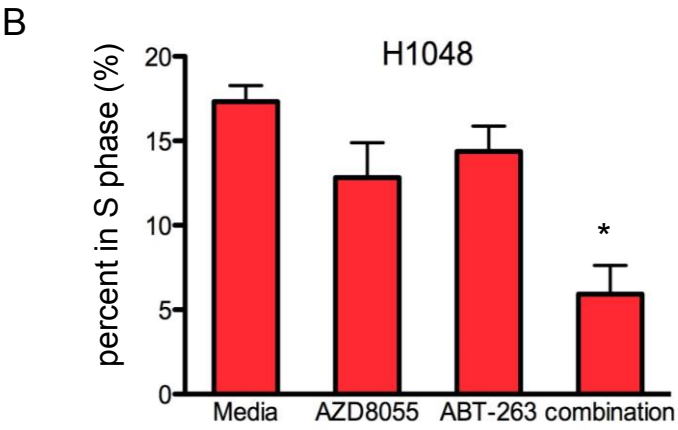

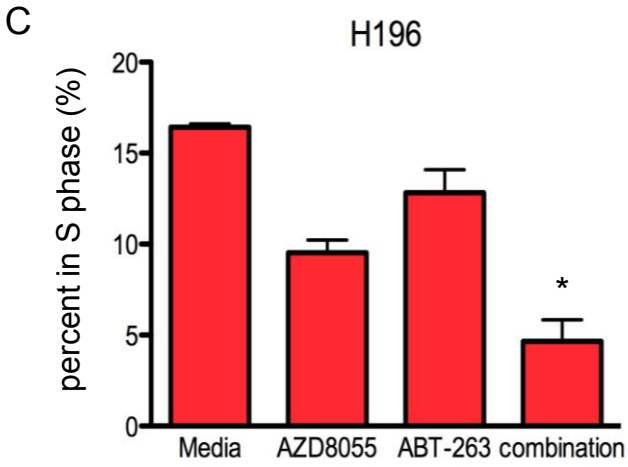

Faber et al. Sup. Figure 7

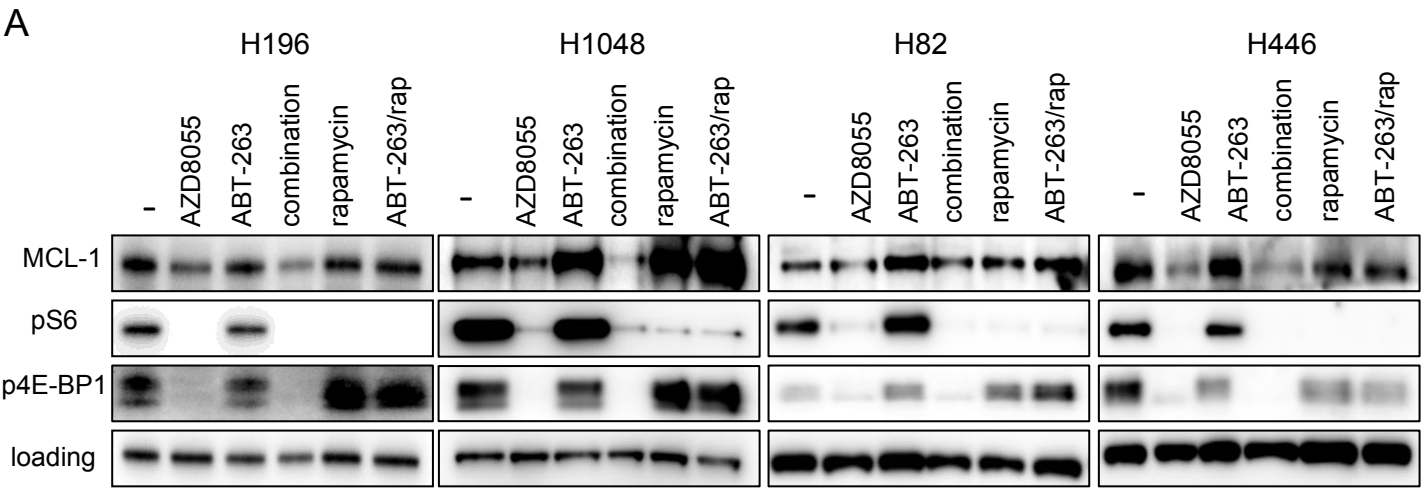

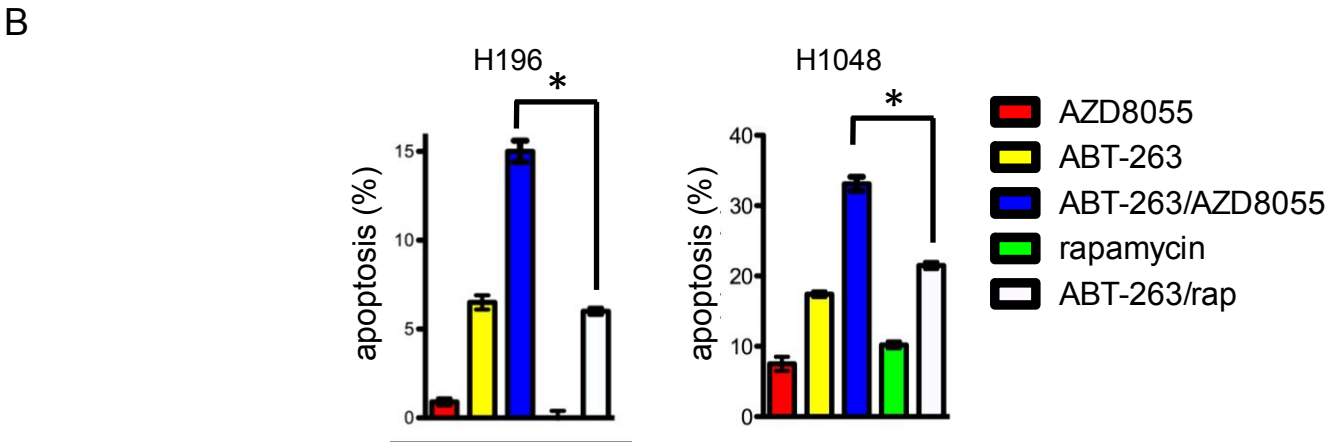

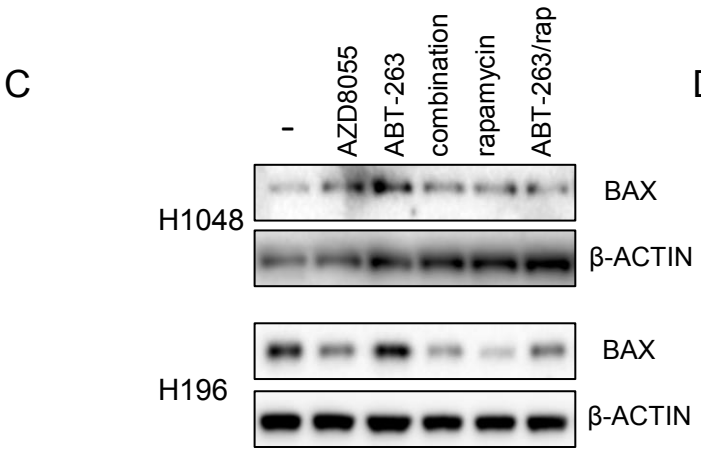

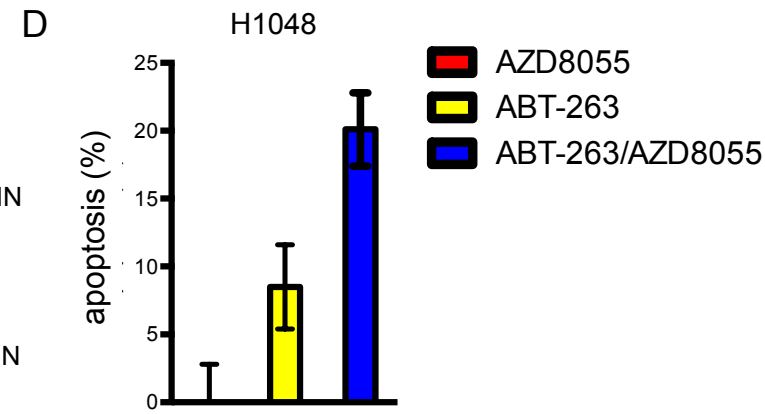

Faber et al. Sup. Figure 8

A

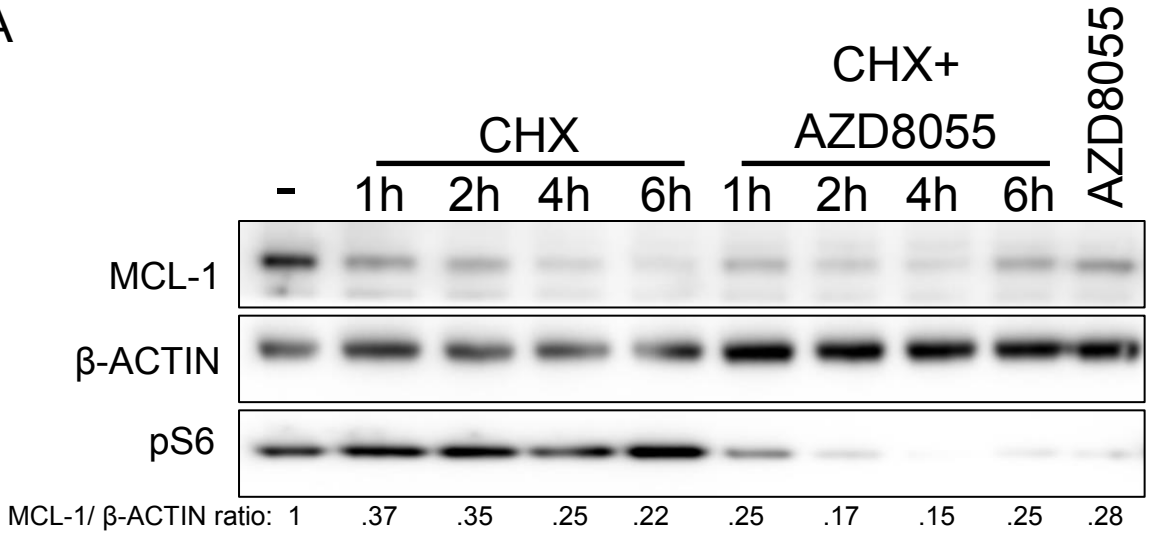

B

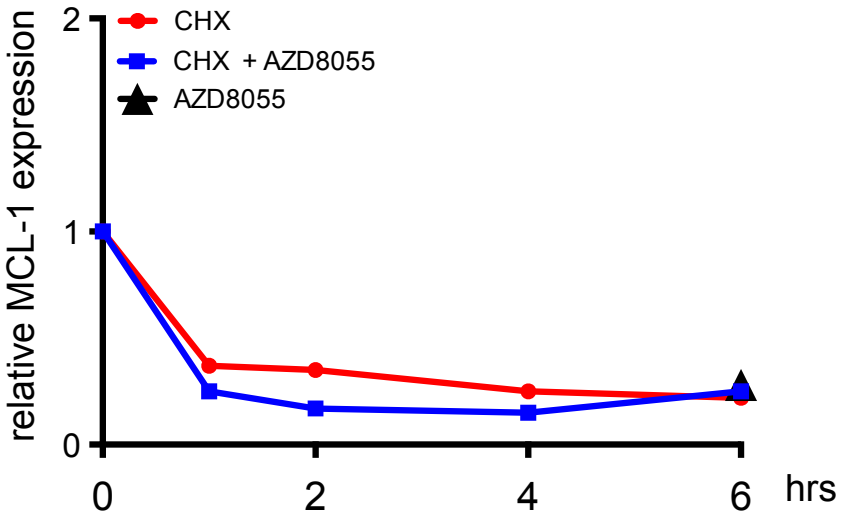

Faber et al. Sup. Figure 9

A

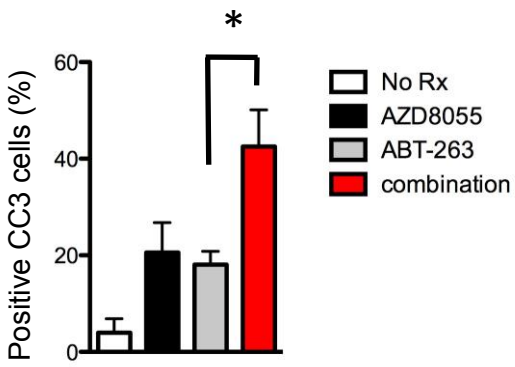

B

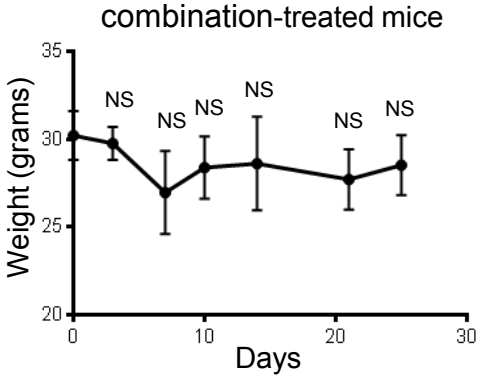

Faber et al. Sup. Figure 10

A

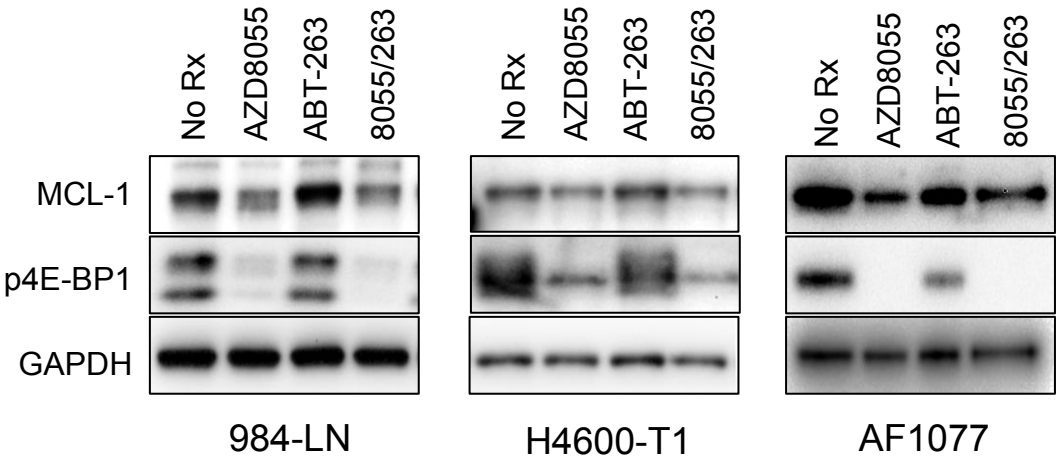

B

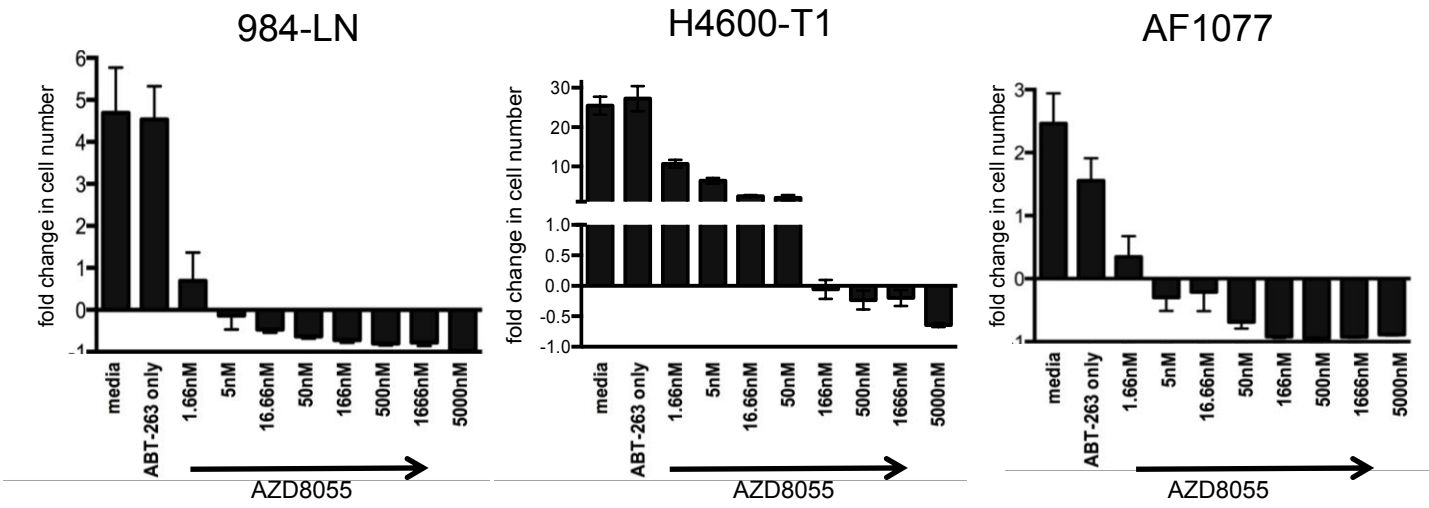

Faber et al. Sup. Figure 11

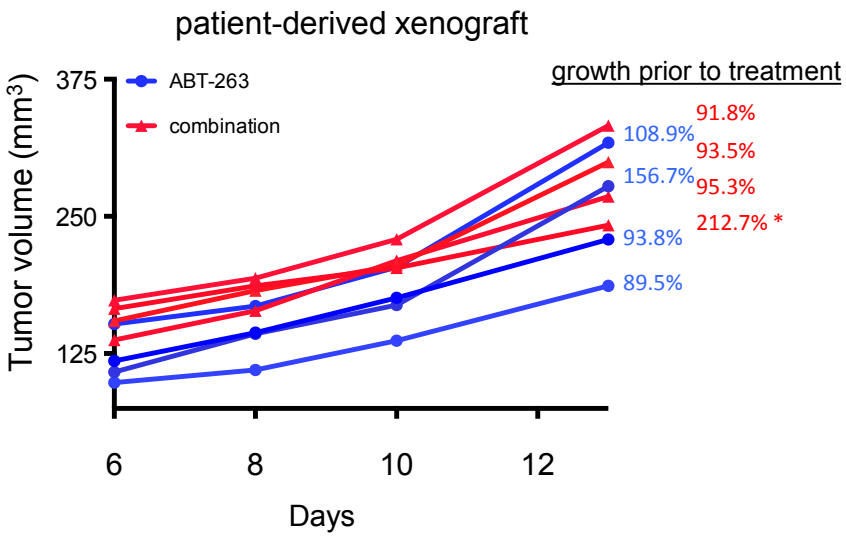

Faber et al. Sup. Figure 12

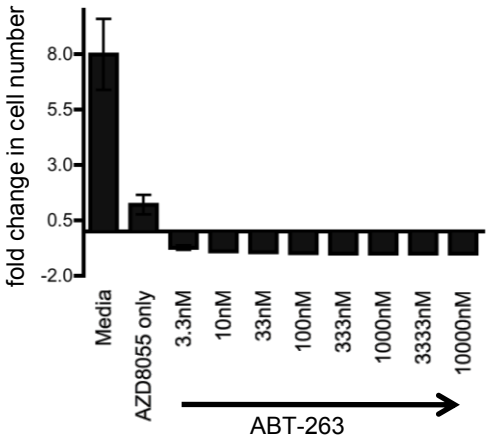

Faber et al. Sup. Figure 13

Supporting Table 1: Autochthonous SCLC GEMM treatments

ear tag	Sex	Virus	Viral titer (PFU x 10^8, per mouse)	Days post-infection - treatment start	Treatment*	Treatment duration (days)	MRI image z axis intervals (mm)	Tumor pre-treatment volume (mm^3)	Tumor post-treatment volume (mm^3)	Tumor volume fold change	Tumor volume percent change
AF1828	M	Ad5-CMV-Cre	2.5	273	ABT	21	0.5	45.9	302.9	6.599	559.9
AF1901	M	Ad5-CMV-Cre	2.0	297	ABT	21	0.5	3.7	19.8	5.319	431.9
AF1216	M	Ad5-CGRP-Cre	5.0	531	ABT	21	1.0	14.1	47.7	3.383	238.3
AF1952	M	Ad5-CMV-Cre	2.2	323	ABT	21	0.5	31.6	76.7	2.427	142.7
AF1965	F	Ad5-CMV-Cre	2.2	274	ABT	21	0.5	6.3	12.8	2.028	102.8
AF1126	M	Ad5-CGRP-Cre	5.0	562	ABT	21	1.0	53.7	20.0	0.372	-62.8
AF1831	F	Ad5-CMV-Cre	2.5	273	ABT/AZD	21	0.5	16.7	28.2	1.689	68.9
AF1960	F	Ad5-CMV-Cre	2.2	323	ABT/AZD	21	0.5	68.1	98.9	1.452	45.2
AF1153	M	Ad5-CGRP-Cre	5.0	532	ABT/AZD	21	1.0	170.0	180.9	1.064	6.4
AF1879	F	Ad5-CMV-Cre	2.0	318	ABT/AZD	21	0.5	8.8	8.5	0.966	-3.4
AF1136	M	Ad5-CGRP-Cre	5.0	562	ABT/AZD	21	1.0	35.7	19.8	0.555	-44.5
AF1833	F	Ad5-CMV-Cre	2.5	273	ABT/AZD	21	0.5	139.4	39.5	0.283	-71.7
AF1829	F	Ad5-CMV-Cre	2.5	273	AZD	21	0.5	2.8	19.0	6.740	574.0
AF1832	M	Ad5-CMV-Cre	2.5	273	AZD	21	0.5	15.9	75.5	4.748	374.8
AF1912	M	Ad5-CMV-Cre	2.2	323	AZD	21	0.5	87.4	397.8	4.551	355.1
AF1894	F	Ad5-CMV-Cre	2.0	367	AZD	21	0.5	59.1	158.9	2.689	168.9
AF1180	M	Ad5-CGRP-Cre	5.0	532	AZD	21	1.0	20.6	39.7	1.927	92.7
MM2579	M	Ad5-CMV-Cre	2.1	293	chemo	28	1.0	74.0	328.8	4.443	344.3
AF1281	F	Ad5-CGRP-Cre	5.0	637	chemo	28	1.0	128.5	389.6	3.032	203.2
AF1488	F	Ad5-CGRP-Cre	5.0	476	chemo	28	1.0	86.8	229.7	2.646	164.6
MM2577	F	Ad5-CMV-Cre	2.1	293	chemo	28	1.0	28.3	35.5	1.254	25.4
AF1400	M	Ad5-CGRP-Cre	5.0	476	chemo	28	1.0	65.6	44.0	0.671	-32.9
AF1899	F	Ad5-CMV-Cre	2.0	367	None	21	0.5	12.2	75.1	6.156	515.6
AF1413	F	Ad5-CGRP-Cre	5.0	589	None	21	1.0, 0.5 **	12.0	56.7	4.725	372.5
AF1162	F	Ad5-CGRP-Cre	5.0	504	None	21	1.0	2.9	10.9	3.759	275.9
AF1093	M	Ad5-CGRP-Cre	5.0	534	None	21	1.0	10.6	24.7	2.330	133.0
MM2520	F	Ad5-CMV-Cre	5.0	434	None	21	0.5	21.0	38.2	1.819	81.9
AF1877	F	Ad5-CMV-Cre	2.0	276	None	21	0.5	12.4	21.6	1.742	74.2
AF1851	F	Ad5-CMV-Cre	2.5	273	None	21	0.5	301.2	329.9	1.095	9.5

* AZD = AZD8055 16 mg/kg PO daily 6 days per week; ABT = ABT-263 80 mg/kg PO daily 6 days per week; ABT/AZD = ABT-263 80 mg/kg PO and AZD8055 16 mg/kg PO daily 6 days per week; chemo = cisplatin 7 mg/kg IP days 1 and 8 and etoposide 10 mg/kg IP days 2 and 9.

** 1 mm z-axis intervals on pre-treatment scan; 0.5 mm z-axis intervals on post-treatment scan